

論文 / 著書情報  
Article / Book Information

Title	Development and performance of an active type shear box in a centrifuge
Authors	Akihiro Takahashi, Jiro Takemura, Akihiro Suzuki, Osamu Kusakabe
Citation	International Journal of Physical Modelling in Geotechnics, Vol. 1, Issue 2, pp. 1-17
Pub. date	2001, 6
DOI	<a href="http://dx.doi.org/10.1680/ijpmg.2001.010201">http://dx.doi.org/10.1680/ijpmg.2001.010201</a>
Note	This file is author (final) version.

## **Development and performance of an active type shear box in a centrifuge**

Takahashi, A.\* , Takemura, J.\*\* , Suzuki, A.\* and Kusakabe, O.\*\*

\* Department of International Development Engineering, Tokyo Institute of Technology, Tokyo, JAPAN

\*\* Department of Civil Engineering, Tokyo Institute of Technology, Tokyo, JAPAN

### **Abstract**

An active type shear box in a geotechnical centrifuge has been newly developed for investigating behaviour of structures subjected to large soil movement. This shear box was designed focusing on deformation of a pile due to lateral movement of soil during earthquake under quasi-static conditions, neglecting inertial effects of soil and pile. The apparatus consists of a laminar box and actuators. With the actuators mounted beside the laminar box, the deformation of the laminar box can be controlled and any ground displacement can be imposed. Even though the deformation of the soil in the box can be controlled as intended, the stress condition of the soil may be different from the ideal condition as in ground motion due to earthquake. Effects of geometry of the shear box and lamina-link mechanism on the deformation and stresses of the soil in the box are investigated with simple finite element analyses. Details of the system are described and the performance of the apparatus in preliminary tests is discussed.

Keywords: laminar box, pile, deformation, earthquake, centrifuge model test, finite element method (IGC: E4/E8/E14)

International Journal of Physical Modelling in Geotechnics 1 (2), 1-17, 2001

Original URL:

<http://dx.doi.org/10.1680/ijpimg.2001.1.2.01>

<http://www.icevirtuallibrary.com/content/article/10.1680/ijpimg.2001.1.2.01>

## 1. INTRODUCTION

Detailed observations on damage of pile foundations after the Hyogoken-Nambu Earthquake of 1995 revealed that damage in piles occurred not only near the top of the piles but also at middle to lower portions of the piles (e.g. Matsui & Oda, 1996, Fujii et al., 1998). The latter damage was mainly found in sites where liquefaction took place and large lateral movements of liquefied soil occurred. In reclaimed land areas, quay walls moved towards the sea and the large ground movement took place due to liquefaction of their foundations and backfill. As a result, many pile foundations near the waterfront were damaged at depths other than pile heads, particularly near the interface between liquefied and non-liquefied soils. Even far from the waterfront, many piles showed similar damage (Tokimatsu & Asaka, 1996) and some of the piles were damaged even without any superstructures (Ohtsu et al., 1997). Furthermore, without the liquefaction of soil, cracks were observed in the middle of piles at some sites (AIJ, 1998). These facts indicate that large deformations took place even in level ground and/or without liquefaction of soils.

The effects of large lateral soil movement, especially liquefaction-induced lateral spreading of soil, on the failure and deformation of the piles have been experimentally investigated using geotechnical centrifuges by many researchers (e.g. Abdoun & Dobry, 1998, Horikoshi et al., 1998, Satoh et al., 1998, Takahashi et al., 1998). In these researches, shaking tables were used to simulate the ground motions during earthquakes. Information derived from the shaking table tests is seen to be of value in demonstrating actual behaviour of piles and soils during earthquakes. However, the actual behaviour of piles is complicated and affected by several factors such as, inertial effect from the superstructure, dynamic response of the soils and the lateral movement of the soils. Investigating the effect of each factor from the complicated behaviour observed in the shaking table tests is not a straightforward process. In order to avoid this complication in the interpretation of the pile behaviour, Tsuchiya et al. (1997) made a new large shearing pit. This shear pit consisted of a huge shear box and actuators. With the actuators mounted beside the shear box, deformation of the shear box could be controlled and any ground displacement could be entered as data input. Using the same concept, the authors developed a new active type shear box in a centrifuge, which makes it possible to simulate the large ground deformation during an earthquake.

This paper focuses on the development of the sophisticated computer controlled active type shear box, which is capable of delivering displacement-controlled deformations to the soil in the shear box and lateral force on top of the pile foundation independently. The details of the shear box are described, and the performance observed in preliminary tests is presented.

## 2. PRELIMINARY CONSIDERATION ON SHEAR BOX

As many researchers have pointed out, soil-pile interaction during earthquake is a highly complicated phenomenon. This research particularly focuses on failure or deformation of the piles due to lateral movement of the soil. Therefore, inertial effects of soil and piles are neglected and quasi-static conditions are assumed. A schematic diagram of active type shear box is shown in [Fig. 1](#). It consists of the following two main parts: a laminar box and four actuators. The shear box was designed for T.I.Tech Mark III centrifuge (Takemura et al., 1999). Due to the limitation of swinging platform space

(0.9×0.9×0.9m) of the centrifuge, only three actuators can be mounted for applying forces to the laminar box. The loading rods of the three actuators are connected to the three laminae at different levels and the lateral force is transmitted to the other laminae through linked vertical thin plate springs. Ideally, in the simulation of ground motion due to earthquake, the laminar box and the soil in it should strain uniformly and uniform stress conditions should be imposed at any level in the horizontal direction as shown in Fig 2(a). However, the stress conditions of soil in the active type shear box are different from the ideal condition. As shown in Fig. 2(b), if the soil is subjected to leftward horizontal displacement at the right boundary, the horizontal normal stress  $\sigma_x$  in the portion near the right end wall would increase being the passive condition, while  $\sigma_x$  in the portion near the left end wall would decrease being the active condition. The variation of  $\sigma_x$  causes the variation of the mean stress as well as the variation of the volumetric strain and shear stress in the horizontal direction.

Although horizontal displacements at the end boundaries can be changed by the three actuators, the displacement profile at the boundaries depends not only on the displacements at the three loading points but also on the deflection of the plate springs. The deflection is determined by the flexural rigidity of the plates and the reaction from the soil to the boundaries. In this section, the effects of the geometry of the shear box, the rigidity of the plate springs on the deformation, and the stresses of the soil in the box are investigated.

### 2.1 Geometry of shear box

To investigate the effect of the geometry of the shear box on the deformation and stress condition of the soil in it, simple two dimensional finite element analyses were carried out under the plane strain condition. In the analyses, the soil was modelled as elastic perfectly plastic employing the extended von Mises yield criteria with non-associated flow rule. The height of the soil in the shear box  $H$  was fixed at 200mm and the width  $W$  was varied from 200 to 800mm, with the aspect ratio  $W/H$  ranging from 1 to 4 in the analyses. Typical FE meshes and the boundary conditions for the analysis are shown in Fig. 3. Triangular-shaped horizontal displacements were monotonically keyed in as input at both side boundaries with a maximum value of 15mm at the top as shown in Fig. 3. Assuming the roughness of the inside surface of the end walls, the vertical displacements of the nodes at both ends were fixed. It was assumed that the shear boxes were deformed under 50 gravities (50-g). With the constitutive law, elastic perfectly plastic model which was used in the analyses, analysed results will be similar at any assumed centrifugal acceleration. As dense Toyoura sand was used in the preliminary tests on the performance of the shear box, the material properties close to those of dense Toyoura sand (Nakamura et al., 1999) were used in the analyses. The dilation angle of the sand is conventionally assumed to be one-third of the frictional angle. The material parameters used in the analyses are summarised in Table 1. Shear modulus was assumed to increase proportionally with depth. Profiles of the vertical stress and shear modulus of the soil are shown in Fig. 4.

Calculated lateral displacement distributions of soil at the central portion of the box at the final stage of the calculation are shown in Fig. 5. The input displacement at the boundary is also plotted as a broken line in the figure. Displacement at the centre decreases with increasing  $W/H$  ratio. The displacement at the centre is almost the same as the input boundary displacement in the case of 200mm-width ( $W/H=1$ ), while for the case where  $W/H=3$  & 4, only 30% & 15% of the input displacement were obtained respectively. From the viewpoint of controlling the deformation of soil, the narrower box is considered

suitable for the tests.

Contours of horizontal normal stress  $\sigma_x$  and shear stress  $\tau_{xz}$  at the maximum input displacement (15mm at the top) are shown in Fig. 6. If the soil behaved as level ground during an earthquake, the contour lines should be horizontal in both  $\sigma_x$  and  $\tau_{xz}$ . In the case of the smallest width ( $W/H=1$ ), the contour lines slanted in the whole area. Since the change of the vertical stresses due to the end-walls friction may not be negligible (Whitman & Lambe, 1986) as shown in this case, it is not good idea not to use the aspect ratio  $W/H=1$  for the tests. However, in the case of larger widths, the contour lines tended to the horizontal around the centre of the box, while they slanted near the end walls. As the model structures, e.g. piles, are normally placed at the centre of the box, it can be said that the use of a wider shear box is better from the viewpoint of the stress condition of the soil. From the above discussions about deformation control and the stress condition of the soil, it could be said that the box with the aspect ratio of 2 to 3 is the best to use for the tests with dense sand and for the situation where strains are not introduced by inertia but by boundary displacement. Since results of the analyses are heavily affected by the constitutive model and parameters of the soil, this aspect ratio may be not applicable for high compressible soil like loose sand. It can be expected that the narrower box is better in the tests with loose sand.

## 2.2 Stiffness of plate springs

In the previous subsection, only the simple shear mode was examined. However, considering real soil deformation due to actual earthquakes, a capability of applying several types of deformation mode to the soil is desirable. For this requirement, the function of plate springs to transmit the force applied by the actuators to the other connected laminae is one of the crucial factors. The effect of the flexural rigidity of the plate spring on the input motion at the end boundaries was investigated here.

Material properties of a spring steel used for plate springs are shown in Table 2. Details of the plate spring connection are shown in Fig. 7. The two sets of plate spring were attached at the each end of the shear box. The set of plate spring consists of several thin steel sheets. It was fixed at the base of the shear box in a hinged condition and held by two cylinder shape holders fixed at each lamina end as shown in the figure. FE analyses were conducted to examine possible maximum displacements of the laminae within the elastic limit of the plate spring. The plate springs with a size of 50mm in width, 300mm in height were assumed in the analyses. Parameters used in the analyses are listed in Table 3. The most severe condition of neglecting the reaction from the soil in the box was assumed and displacements of these modes were imposed to the beam at three different levels corresponding to those of the actuators. Typical FE meshes and the boundary conditions for analysis are shown in Fig. 8. The most severe input displacement assumed is shown in Fig. 9.

Calculated deflection and bending moment distributions of the plate are shown in Fig. 10. Bending moments at yielding are also shown as broken lines. As shown in Fig. 10, the maximum deflection of the plate springs with thinner steel sheets and more sheets within the elastic limit is larger than that with thicker sheets and less sheets. On the other hand, when the beam is subjected to lateral distributed load like earth pressures, the deflection of the beam between the points of loading by the actuators becomes larger for the former springs than the latter. In order to satisfy the non-yielding and less deflection conditions with the same total thickness of the plate springs, both flexibility and rigidity are required for the plate springs. It is very difficult to find the optimum combination of the thickness of the spring sheet

and the number of layered sheets for the spring plates. However, considering the fact that the tests will be done under 50-g or 100-g and 20 millimetres in displacement is large enough in terms of displacement of pile, the analysed condition with the high rigidity seems to be a better condition.

### 3. SYSTEM DESCRIPTION

The active type shear box was designed to fit the 0.9-by-0.9m swinging platform of the Mark III Centrifuge at T.I.Tech. Side view of the active type shear box and the box mounted on the centrifuge are shown in Fig. 11. The shear box was designed to be operational under 100-g. The shear box can be disassembled into two parts: the laminar box and the actuators.

The laminar box was made of duralumin (aluminium 2017) with inner size of 450mm in width, 200mm in breadth and 325mm in height. If the soil below two-thirds of the model depth is a bearing stratum of a pile foundation, the aspect ratio of the shear zone will be 2.3 ( $=450\text{mm}/200\text{mm}$ ), which falls within the suggested range of 2 to 3 in the previous section. The box consists of thirteen-stacked 24mm-thick alumite coated duralumin laminae. The outer size of the lamina is W512×B262×H24mm and the inner size is W452×B202×H24mm. The laminae are supported by roller bearings, which are mounted in grooves on each lamina. To prevent the movement perpendicular to the loading direction, four external columns with rollers are placed just outside of the box as shown in Fig. 11(a). A rectangular shape rubber sheeve is placed in the box to inhibit soil particles from getting in to the gaps between the laminae. Thin aluminium shear sheets roughened by glued Toyoura sand lie just inside both end walls and are fixed to the base of the box. These sheets are for developing shear stresses on the vertical contact surface with the soil. The three actuators are connected with the three laminae directly and lateral forces are transmitted to the other laminae through four linked sets of thin plate springs. Each thin plate spring consists of three-layers of 0.6mm-thick or six-layers of 0.3mm-thick spring steel sheets. Detail of the plate spring connection to the laminae is as shown in Fig. 7.

Four Servo-Technos Model L9714 linear hydraulic actuators are attached to steel racks as shown in Fig. 11(a). The actuator at the top is used for simulating lateral force acting on the pile head. The bottom three actuators have a stroke of  $\pm 20\text{mm}$ ; the top one has that of  $\pm 40\text{mm}$ . All actuators have piston areas of  $1260\text{mm}^2$  and  $880\text{mm}^2$ , force capacities of 25.8kN and 18.0kN at 20.5MPa oil pressure when moving outward and inward, respectively. The servo-valve used for each actuator is MOOG J076-101. The peak velocity of the actuator is 133mm/sec. A servo control box is mounted on the centrifuge. A PC in the control room of the centrifuge communicates with the on-board PC installed in the control box through slip rings of the centrifuge. Signals from the on-board PC are fed to the servo valve to give the actuating piston displacements. A closed loop feedback system is built by using the signals collected by linear variable differential transformers (LVDTs) attached on the actuators. The actuator for the pile head loading can also be controlled by a load cell attached on the rod of the actuator. A schematic drawing of the hydraulic circuit is shown in Fig. 12. Pressurised oil is supplied by a hydraulic pump placed on the laboratory floor. A rotary joint with maximum pressure of 20.5MPa mounted on the centrifuge is used for charging and discharging oil to the centrifuge during spinning of the centrifuge. Two four-litre hydraulic accumulators are mounted on the centrifuge to satisfy the required flow rate of the pressurised oil. With these accumulators, the four actuators can be manipulated at a frequency of 1Hz with the double amplitude of horizontal displacement of 20mm. Specifications of the active type



shear box are summarised in [Table 4](#).

#### 4. RESULTS OF PRELIMINARY TEST ON PERFORMANCE OF THE SHEAR BOX

A series of preliminary tests was carried out to examine the characteristics of the empty shear box and to observe the deformation of the soil in the shear box and pile behaviour when subjected to large soil deformation. [Figure 13](#) illustrates the instrumentation used in the tests. Horizontal displacements of six laminae in the stacks were measured by LVDTs at the mid-portion of the box. Displacements of the actuator rods were also measured using LVDTs. In the cases for the box filled with soil, aluminium markers were placed in the soil during preparation. Positions of the makers were scaled before and after the tests to measure the deformation of the soil. In the tests with model pile foundation, strain gauges were attached inside of the pile at ten different levels. Deflections and angles of the pile head were also measured by two laser displacement transducers.

##### *4.1 Performance of the active type shear box*

As a first series of preliminary tests, proof tests on the empty shear box were carried out at 1-g and 25-g to make a comparison between the input displacements by the actuators and the measured displacements of the laminae using the LVDTs. Since the reliability of the control box on the centrifuge in high centrifugal acceleration at the time of preliminary tests was low, the centrifugal acceleration was set at 25-g, although the shear box was designed to be operational under 100-g. Test conditions are listed in [Table 5](#). Two types of shear deformation mode were assumed as shown in [Fig. 14\(a\)](#). The distributions of shear modulus corresponding to these two modes are shown in [Fig. 14\(b\)](#). One is a first natural vibration mode for level ground with its shear velocity or shear modulus uniform throughout the depth. The other is another first mode for level ground with a shear velocity that increases with depth. The former mode is referred as 'Type A' and the latter one is referred as 'Type B,' following the foundation design codes for railway structures in Japan (RTRI, 1997). In Cases EA1 & EA2, Type A mode was used while Type B mode was used in the others cases. In the test series, the thickness of the spring sheet used for the plate springs was 0.6mm. For each spring plate, 3 layered sheets were used. Sinusoidal waves with a period of 30 seconds were applied to the laminae. [Figure 15](#) shows the typical time histories of the actuator rod displacement. Observed horizontal displacement distributions of the laminae when the displacement of the top lamina reached 5, 10 and 15mm are shown in [Fig. 16](#). In all the cases, measured displacement of the laminae closely approximates the input motion regardless of the centrifugal acceleration. This implies that frictions between laminae did not significantly affect the performance of the shear box.

A separate series of tests for the shear box filled with dense sand was performed at 25-g. Toyoura sand with relative density of 80% was used for the model ground. The mean grain size of Toyoura sand is 0.2mm and the coefficient of uniformity is approximately 1.6. [Table 6](#) shows the test conditions of this series. The shear deformation mode of the soil in Cases FA1 & FA2 is Type A and that in Cases FB1 & FB2 is Type B, respectively. In Cases FA2 & FB2, the soil below two-thirds of the model depth was assumed to be a bearing stratum and the input displacement was applied only to the upper two-thirds of the model. During earthquake, the soil may move and affect the response of the pile even at the depth corresponding to the lowest one-third of the box. In the application of the box to the soil-pile interaction

problem, the pile foundation was not assumed a friction pile but an end bearing pile in this study as would be described in detail at a latter section. Though the end bearing pile can be modelled by fixing the pile tip on the base of the box, it is not a realistic boundary condition for the pile. For that reason, the lowest one-third of the soil was assumed to be the bearing stratum. In this series, two types of plate springs were used. One consisted of three-layers of 0.6mm-thick spring steel sheets and the other consisted of six-layers of 0.3mm-thick sheets. In Case FB1, the spring plates of three-layers of 0.6mm-thick steel sheets were used. The former plate spring had four times the flexural rigidity of the latter one. A single quarter cycle of a sinusoidal wave was applied to the laminae in 120 seconds.

Distributions of the horizontal displacement of the laminae measured by LVDTs at the centre of the box, when the displacement of the top lamina reached 1/3, 2/3 and 1 of the maximum input displacements, are shown in Fig. 17. The displacements of the laminae to which the actuators were directly connected showed a good agreement with the target displacements (input motion by the three actuators) which is shown by broken lines. The non-direct-connected laminae on the other hands did not attain the target displacements resulting to many kinks in the distributions. Figure 18 shows the displacement distributions of the laminae normalised by the target value. The difference between the measured displacements and the input values is smaller for the plate springs with higher flexural rigidity than for those with smaller rigidity. As shown in Fig. 17, the difference between the target and observed displacements does not proportionally increase with the target displacements. Particularly for FB1 and FB2, the difference developed mainly in the first 5mm displacement at the top lamina and there was little increase of the difference in the rest of the shearing process. As a result, the smaller target displacement is the smaller normalised displacement.

Distributions of the horizontal ground displacements measured with the targets placed at the centre of the model ground are compared with those of the laminae and the target values at the end of shearing. These comparisons are shown in Fig. 19. In this figure, only the displacements for the cases with large flexural rigidity plate springs ( $t=0.6\text{mm}$ ,  $n=3$ ) are illustrated. Observed distributions of the ground displacement at the centre of the model were similar to the input values in all the cases and the distribution of the ground displacement is smoother than that of the laminae. Figure 20 shows the ground displacement distributions normalised by the target values at the end of the shearing. Although in Cases FB1 and FB2, there is a large fluctuation in the lower portion where the displacements of the laminae are small, the ground displacement becomes almost 70~80% of the input value in all the cases. The ratio of the ground displacement to the input displacement from the side end is close to the FE analysis results for the cases with similar aspect ratios. As stress conditions in the ground are complex and different from those that occur during earthquakes as discussed in Section 2. These should be taken into account and examined by numerical analyses in the interpretations of the test results obtained from this apparatus.

#### *4.2 Preliminary tests on soil-pile interaction*

Preliminary tests on a passive single pile were carried out under 25-g to examine the capability of this apparatus and investigate the behaviour of the pile in a large soil movement, specifically the soil-structure interaction during an earthquake. Experimental researches on the passive pile, especially on an arching effect and a pile group effect, have been previously conducted by several researchers (Wang & Yen, 1974, Matsui et al., 1982, Chen et al., 1997). In this test series, behaviour of piles subjected to two types of



large soil deformations was observed. The effect of rigidity of the plate springs, which may govern the deformation of soil in the box, on the deformation of the pile was examined. In the tests, the stainless steel-made model pipe pile, the properties of which are listed in Table 7, was placed in the box as shown in Fig. 13. The diameter of the pile was 75 times as large as the mean diameter of the Toyoura sand and was large enough to conduct the pile loading tests (Garnier & König, 1998). The surface of the model pipe pile was smooth. The pile tip was installed into the bearing stratum, which is the lowest one-third of the soil. Imposed soil deformation modes on the box were Type A and Type B, which were the same modes as FA2 and FB2 in the previous section. Test conditions of this test series are shown in Table 8. In Cases PA1 and PB1, only one cycle sinusoidal motion was applied to the laminae in 480 seconds. In Cases PA1C and PA2C, 120-second cycle sinusoidal motions were applied to the laminae, where the peak values of the applied waves were increased after applying three cycles, up to 15mm at the top lamina. Figure 21 shows typical time histories of the input displacement by the actuators in Case PA2C.

The relationship between observed displacements at the pile head and the input displacements of the lamina at the ground surface for all the cases are shown in Fig. 22. It should be noted that the displacements of the pile at the pile head shown in the figure were measured at the target 50mm above the surface of the ground as shown in Fig. 13. In all the cases, the relationship shows non-linearity, especially in the cases with flexible plate springs (PA1, PA1C and PB1). As the piles did not show yielding in all the cases, these non-linear relations are attributed to the non-linear response of the soil. Figure 23 shows observed bending strain distributions of the pile when the displacement of the top lamina reached 3, 9 and 13mm for the first time in the sequences of the box shearing. The flexibility of the plate springs is expected to affect the deformation of the soil in the box. However, according to the observed bending strain distributions of the pile in Cases PA1 and PA2 with different flexural rigidities of the plate springs, the effect of the flexural rigidity of the springs on the soil deformation appears to be insignificant at the centre of the shear box.

In all the cases, maximum bending strain can be seen at the depth of 200mm (the height of 100mm) that corresponds to the interface between the less deformed bearing stratum and the sheared soil. These results agree with those obtained by Poulos et al. (1995) in their small model tests. In their tests, only the triangular displacement distribution could be applied to the soil. Regarding the difference in the input deformation mode, the maximum displacement of Case PB1 at the pile head is smaller than that of Case PA1 as shown in Fig. 22. These two cases also differ in the bending strain distributions of the pile as shown in Fig. 23. As shown in Fig. 19, the ground displacement at the centre is not so sensitive to the boundary conditions and the difference with the deformation mode of the soil at the centre cannot be clearly seen in the ground displacement in the comparison between Cases FA2 and FB2. However, there is an obvious difference in the response of the pile as shown in Fig. 22 and Fig. 23. This shows that the response of the pile is very sensitive to the ground displacement or the type of ground motion.

Although further improvement of the apparatus is needed in order to interpret the test results properly, especially for the measurement of the actual ground displacement, it can be concluded that this apparatus could be a valuable tool for studying the soil-structure interaction during earthquakes. The differences should be taken into account for the interpretation of test results.

## 5. INTERPRETATION OF TEST RESULTS AND FURTHER APPLICATIONS

The observed distributions of the ground displacement at the centre of the model were similar to the input motions and it became almost 70~80% of the input value as shown in the previous section. This fact indicates that the active type shear box has adequate capability in the modelling of the intended strain fields in the soil. However, the soil deformation was mainly caused by lateral normal stresses rather than shear stresses, according to the numerical analyses in Section 2. Hence, the stress condition generated by the shear box is different from the free-field stress situation in earthquakes. Given such limitation, the obtained test results for earthquake problems cannot be directly applicable to practical problems. However, one of the aims of this application in the soil-pile interaction problems during earthquakes is to observe the response of the pile in the different types of soil movements. The test results discussion in Section 4.2 showed that the response of the pile was very sensitive to the mode of ground movement. Therefore, this system can provide useful data for verification of the numerical analyses. It should be noted that the stress conditions in the soil and the soil displacements, e.g. vertical and normal stresses in the soil and the displacement of the soil around the targeted structure, must be measured in the tests for verification. In the Japanese seismic design code for railway structures (RTRI, 1997), it is prescribed that the displacements of the pile foundation during earthquakes should be assessed by the beam structure analyses subjected to soil movements through soil springs. The active type shear box tests also have the capability to fulfil such requirement of the seismic design code.

Although only the application of the active type shear box to the soil-pile interaction during earthquakes was introduced in this paper, it can be used for a problem in which modes of horizontal ground movement play an important role. For instance, assuming that the end walls of the laminar box is a flexible retaining wall and the soil in the box is a surrounding ground at an excavation site, various modes of the wall deflection can be simulated with the mounted actuators. This kind of tests makes it possible to investigate the effect of wall deflection mode on the earth pressure and the deformation and settlement of the ground at the retained side.

## 6. CONCLUDING REMARKS

In this study, the active type shear box in the centrifuge has been newly developed for investigating the behaviour of structures subjected to large soil movement. The effects of the configuration of the shear box were investigated with simple finite element analyses. Details of the system were described and performance of the apparatus in preliminary tests was discussed. The following conclusions are derived:

- (1) Considering both deformation control and stress conditions of soil, the laminar box with the aspect ratio of 2 to 3 is better to use for the tests with dense sand, based on the simple two dimensional finite element analysis results.
- (2) Tests on the empty shear box were carried out at 1-g and 25-g and it was confirmed that frictions between laminae were not significant on the performance of the shear box.
- (3) The displacements of the laminae to which the actuators were directly connected showed quite good agreement with the target displacements, though the non-direct-connected laminae did not attain the target displacements resulting to many kinks in the distributions in the tests for the shear box filled with dense Toyoura sand. However, the observed distributions of the ground displacement at the centre of the model were similar to the input motions. The ground displacement at the centre of the model became almost 70~80% of the input value and they were smoother than those of the laminae

were.

- (4) The effect of flexural rigidity of the plate springs, which were attached to the ends of the laminar box to transmit applied lateral displacements from the actuators to all the laminae, on the pile deformation was examined. Results showed that the effect of the rigidity of the springs on the soil and pile deformation was not significant.
- (5) Behaviour of piles subjected to two types of large soil deformations was observed. It was observed that the response of the pile is very sensitive to the ground displacement or the type of ground motion.

## ACKNOWLEDGEMENT

The authors gratefully acknowledge the funding for this research provided by the Ministry of Education, Science, Sports and Culture, Japan. The first author would also like to express his gratitude to the Department of Civil Engineering, Tokyo Institute of Technology for its financial and logistical support

## REFERENCES

- Abdoun, A. & Dobry, R. (1998): "Seismically induced lateral spreading of two-layer sand deposit and its effect on pile foundations," *Proceedings of the International Conference Centrifuge 98*, Vol.1, 321-328
- Architecture Institute of Japan (1998): Report on the Hanshin-Awaji Earthquake Disaster, Building Series Volume 4, Building Foundations, 463-465 (in Japanese)
- Chen, L.T., Poulos, H.G. & Hull, T.S. (1997): "Model tests on pile groups subjected to lateral soil movement," *Soils and Foundations*, Vol. 37, No. 1, 1-12
- Fujii, S., Iseimoto, N., Satou, Y., Kaneko, O., Funahara, H., Arai, T. & Tokimatsu, K. (1998): "Investigation and analysis of a pile foundation damaged by liquefaction during the 1995 Hyogoken-Nambu Earthquake," *Soils and Foundations, Special Issue on Geotechnical Aspects of the Jan. 17 1995 Hyogoken-Nambu Earthquake*, No. 2, 179-192
- Garnier, J. & König, D. (1998): "Scale effects in piles and nails loading tests in sand," *Proceedings of the International Conference Centrifuge 98*, Vol.1, 205-210
- Horikoshi, K., Tateishi, A. & Fujiwara, T. (1998): "Centrifuge modeling of a single pile subjected to liquefaction-induced lateral spreading," *Soils and Foundations, Special Issue on Geotechnical Aspects of the Jan. 17 1995 Hyogoken-Nambu Earthquake*, No. 2, 193-208
- Matsui, T., Hong, W.P. & Ito, T. (1982): "Earth pressures on piles in a row due to lateral soil movements," *Soils and Foundations*, Vol. 22, No. 2, 71-81
- Matsui, T. & Oda, K. (1996): "Foundation damage of structures," *Soils and Foundations, Special Issue on Geotechnical Aspects of the Jan. 17 1995 Hyogoken-Nambu Earthquake*, No. 1, 189-200
- Nakamura, Y., Kuwano, J. & Hashimoto, S. (1999): "Small-strain stiffness and creep of Toyoura sand measured by a hollow cylinder apparatus," *Proceedings of Pre-Failure Deformation of Geomaterials*, Vol. 1, 141-148
- Ohtsu, H., Hatsuyama, Y., Tateishi, A. & Horikoshi, K. (1997): "A study on pile foundations damaged by the 1995 Hyogoken Nambu Earthquake," *Proceedings of International Conference on Deformation and progressive failure in geomechanics*, 583-588
- Poulos, H.G., Chen, L.T. & Hull, T.S. (1995): "Model tests on single piles subjected to lateral soil

- movement,” *Soils and Foundations*, Vol. 35, No. 4, 85-92
- Railway Technical Research Institute (1997): “Seismic design for foundations,” *Foundation design codes for railway structures*, 116-117 (in Japanese)
- Satoh, H., Ohbo, N. & Yoshizako, K. (1998): “Dynamic test on behavior of pile during lateral ground,” *Proceedings of the International Conference Centrifuge 98*, Vol.1, 327-332
- Takahashi, A., Takemura, J., Kawaguchi, Y., Kusakabe, O. & Kawabata, N. (1998): “Stability of piled pier subjected to lateral flow of soils during earthquake,” *Proceedings of the International Conference Centrifuge 98*, Vol.1, 365-370
- Takemura, J., Kondoh, M., Esaki, T., Kouda, M. & Kusakabe, O. (1999): “Centrifuge model tests on double propped wall excavation in soft clay,” *Soils and Foundations*, Vol. 39, No. 3, 75-87
- Tokimatsu, K. & Asaka, Y. (1998): “Effects of liquefaction-induced ground displacements on pile performance in the 1995 Hyogoken-Nambu Earthquake,” *Soils and Foundations, Special Issue on Geotechnical Aspects of the Jan. 17 1995 Hyogoken-Nambu Earthquake*, No. 2, 163-177
- Tsuchiya, T., Kikuchi, D., Yamada, T., Kakurai, M. & Yamashita, K. (1997): “Lateral loading tests on the model pile in the large scale shearing pit considering deformation of pile top and ground,” *Proceedings of the 32nd Japan National Conference on Geotechnical Engineering*, 1545-1548 (in Japanese)
- Wang, W.L. & Yen, B.C. (1974): “Soil arching in slopes,” *Journal of the Geotechnical Engineering Division, ASCE*, Vol. 100, GT1, 61-78
- Whitman, R.V. & Lambe, P.C. (1986): “Effect of boundary conditions upon centrifuge experiments using ground motion simulation,” *Geotechnical Testing Journal, GTJODJ*, Vol. 9, No. 2, 61-71

**Table 1** Material parameters used in analyses

Shear modulus at $p'=98\text{kPa}$	175 MPa
Poisson's ratio : $\nu$	0.33
Frictional angle : $\phi$	40 deg.
Dilation angle : $\psi$	13.3 deg. (one third of frictional angle)
Coefficient of earth pressure at rest : $K_0$	0.5
Unit weight at 50-g : $\gamma_{50}$	770 kN/m <sup>3</sup>

**Table 2** Material properties of spring steel

Name	SUP3, hardened
Young's modulus	206 GPa
Poisson's ratio	0.24
Yield strength	More than 835 MPa

**Table 3** Analysis parameters

Case	Thickness of a steel sheet: $t$ (mm)	Number of layered sheets: $n$	Flexural rigidity of plate spring (N.m <sup>2</sup> )	Maximum input displacement (mm)
P1	0.3	6	0.14	35.5
P2	0.6	3	0.56	17.8

**Table 4** Specifications of the active type shear box

Maximum operational centrifugal acceleration		100-g
Actuator	Number	3 for laminar box, 1 for pile head
	Stroke	$\pm 20\text{mm}$ for laminar box, $\pm 40\text{mm}$ for pile head
	Force capacity at 20.5MPa oil pressure	25.8kN for outward, 18.0kN for inward
	Peak velocity	133mm/sec
Laminar box	Number of stacks	13
	Inner size	W450×B200×H325mm
	Flexural rigidity of plate spring: $EI$	0.14N.m <sup>2</sup> , 0.56N.m <sup>2</sup>

**Table 5** Test conditions for the empty shear box

Case	Centrifugal acceleration (g)	Maximum displacement amplitude of actuators (mm)		
		Actuator L	Actuator M	Actuator U
EA1	1	7.5	13.0	15.0
EA2	25	7.5	13.0	15.0
EB1	1	3.7	8.6	15.0
EB2	25	3.7	8.6	15.0

**Table 6** Test conditions for the shear box filled with dense sand

Case	Centrifugal acceleration (g)	Maximum displacement amplitude of actuators (mm)		
		Actuator L	Actuator M	Actuator U
FA1-F, R	25	8.8	15.2	17.5
FA2-F, R	25	0.0	10.6	15.0
FB1-F,	25	4.6	9.8	17.5
FB2-F, R	25	0.0	6.0	15.0

\* F:  $t=0.3\text{mm}$ ,  $n=6$ , R:  $t=0.6\text{mm}$ ,  $n=3$  for plate spring

**Table 7** Properties of model pipe pile

Young's modulus : $E$	210 GPa
Thickness of pipe : $t$	0.50 mm
Cross-sectional area : $A$	$2.28 \times 10^{-5} \text{ m}^2$
Centroidal moment of inertia : $I$	$5.99 \times 10^{-10} \text{ m}^4$

**Table 8** Test conditions for single passive pile tests

Case	Thickness of a steel sheet (mm)	Number of layered steel sheets	Displacement amplitude of actuators (mm)		
			Actuator L	Actuator M	Actuator U
PA1	0.3	6	0.0	9.3	14.0
PA1C	0.3	6	0.0	2.0	3.2
				6.1	9.4
				10.6	15.0
PA2C	0.6	3	0.0	2.0	3.2
				6.1	9.4
				10.6	15.0
PB1	0.3	6	0.0	5.8	13.2



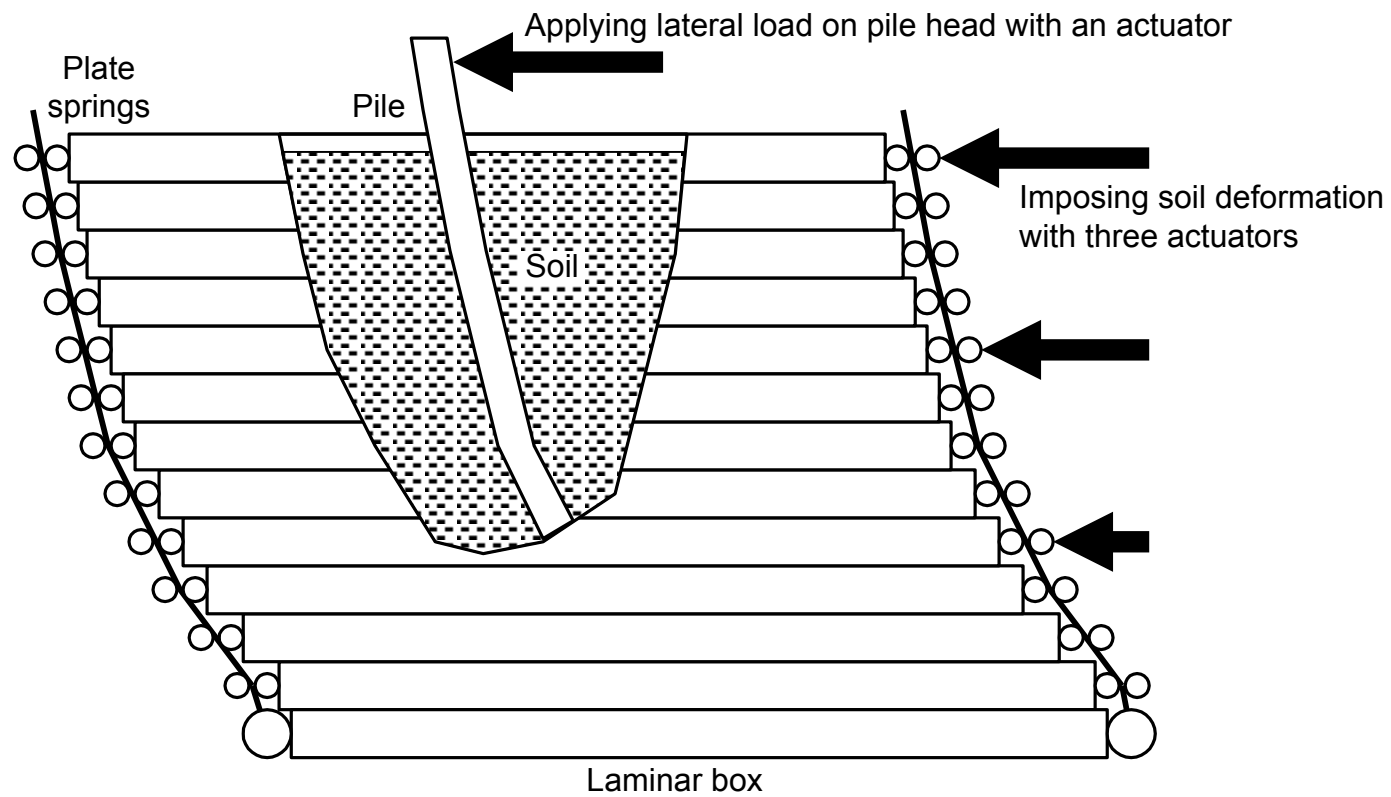


Figure 1 A schematic diagram of an active type shear box

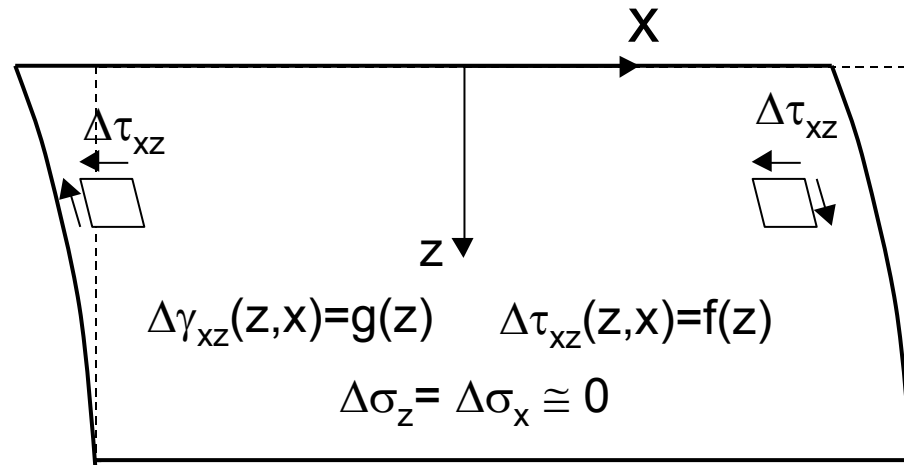


Figure 2(a) Ideal deformation of level ground due to earthquake

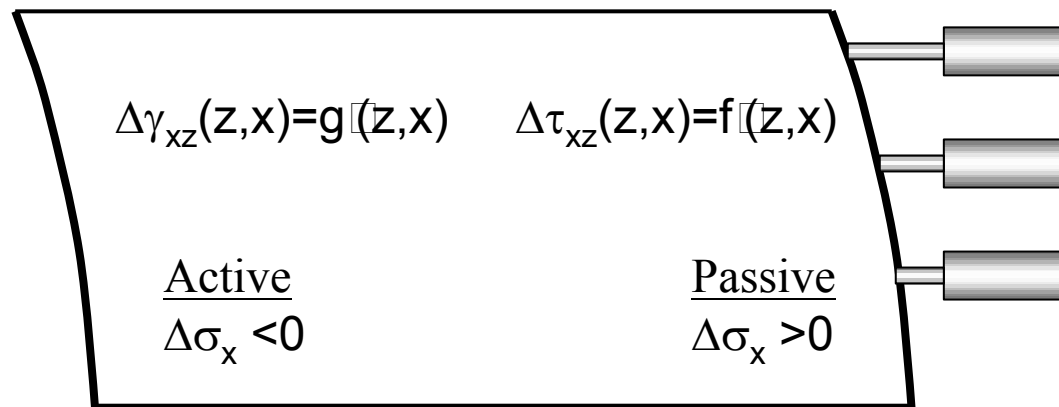


Figure 2(b) Variation of stress and strain in active type shear box

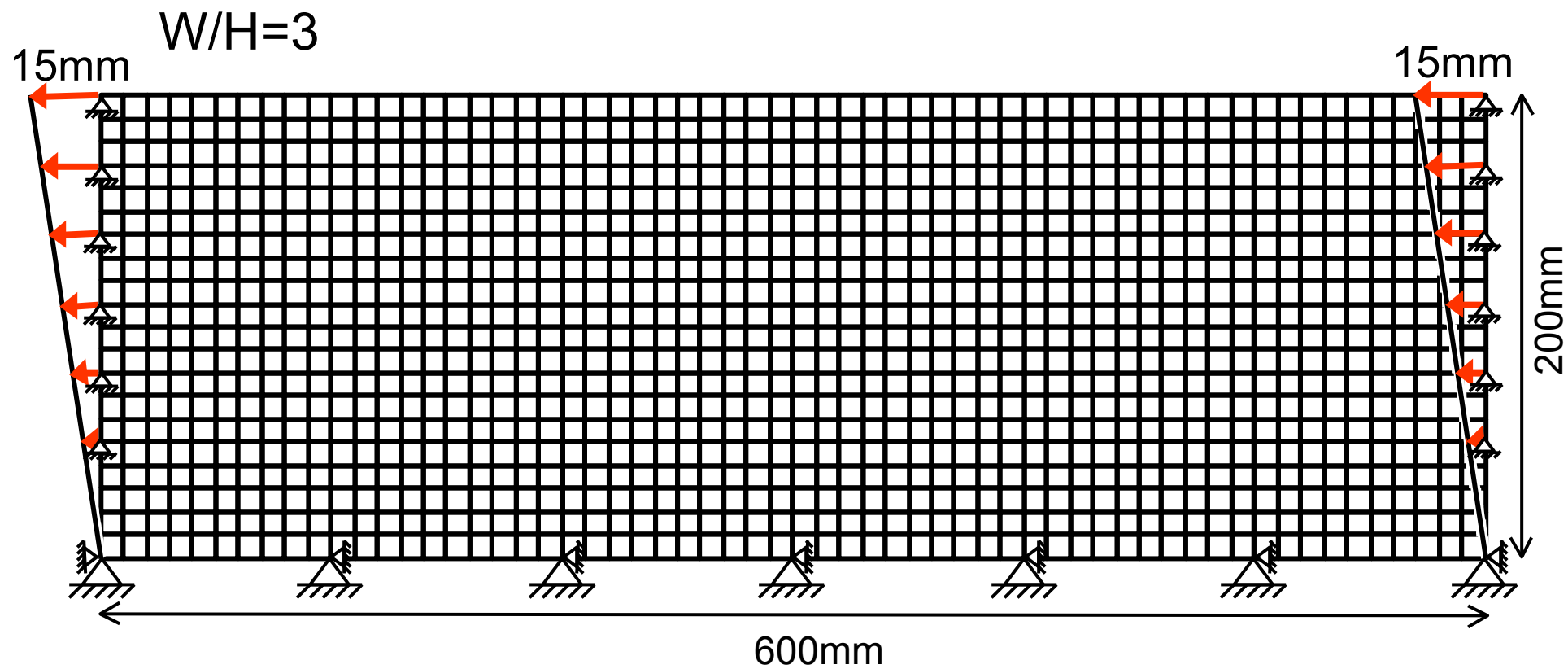


Figure 3 Typical FE mesh and the boundary condition for analysis

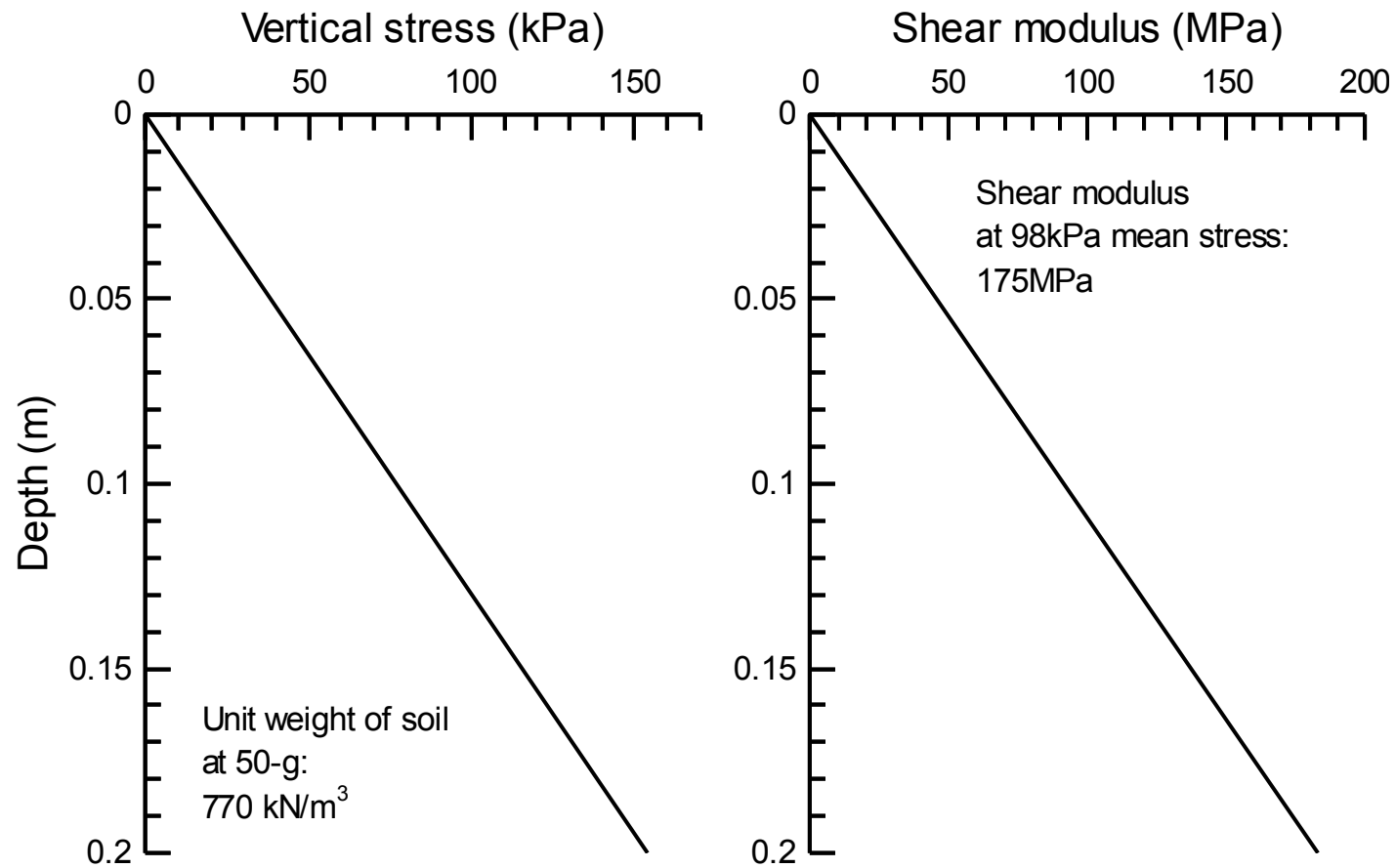


Figure 4 Profiles of the vertical stress and shear modulus of the soil

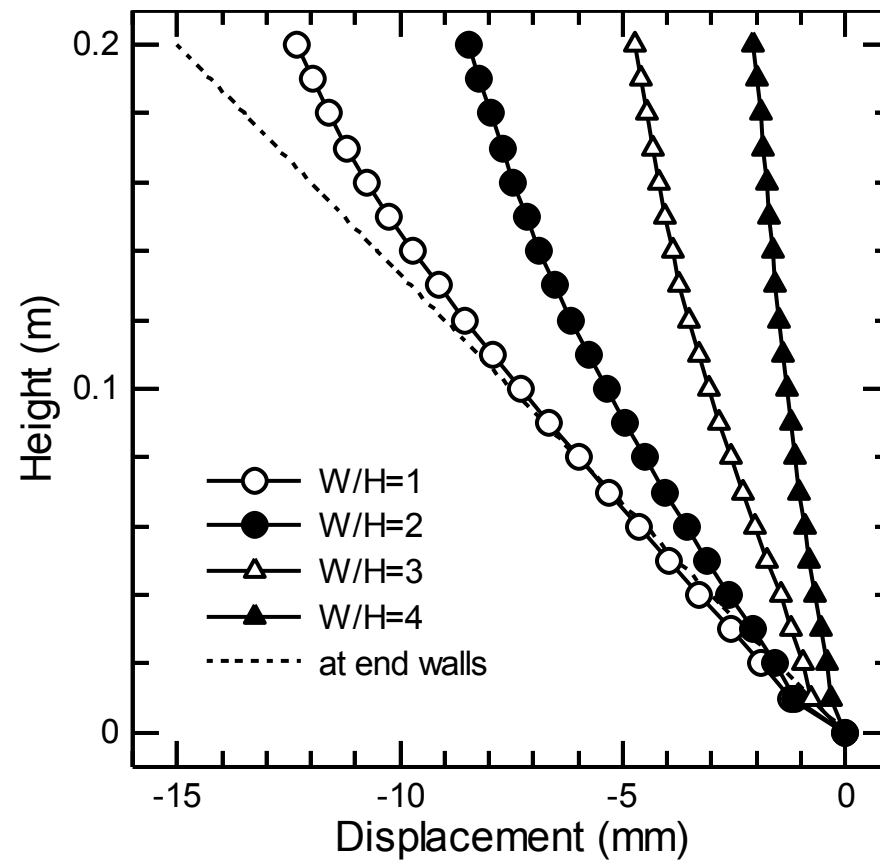


Figure 5 Calculated lateral displacement distributions of the soil at the centre of the box at the final stage of calculations

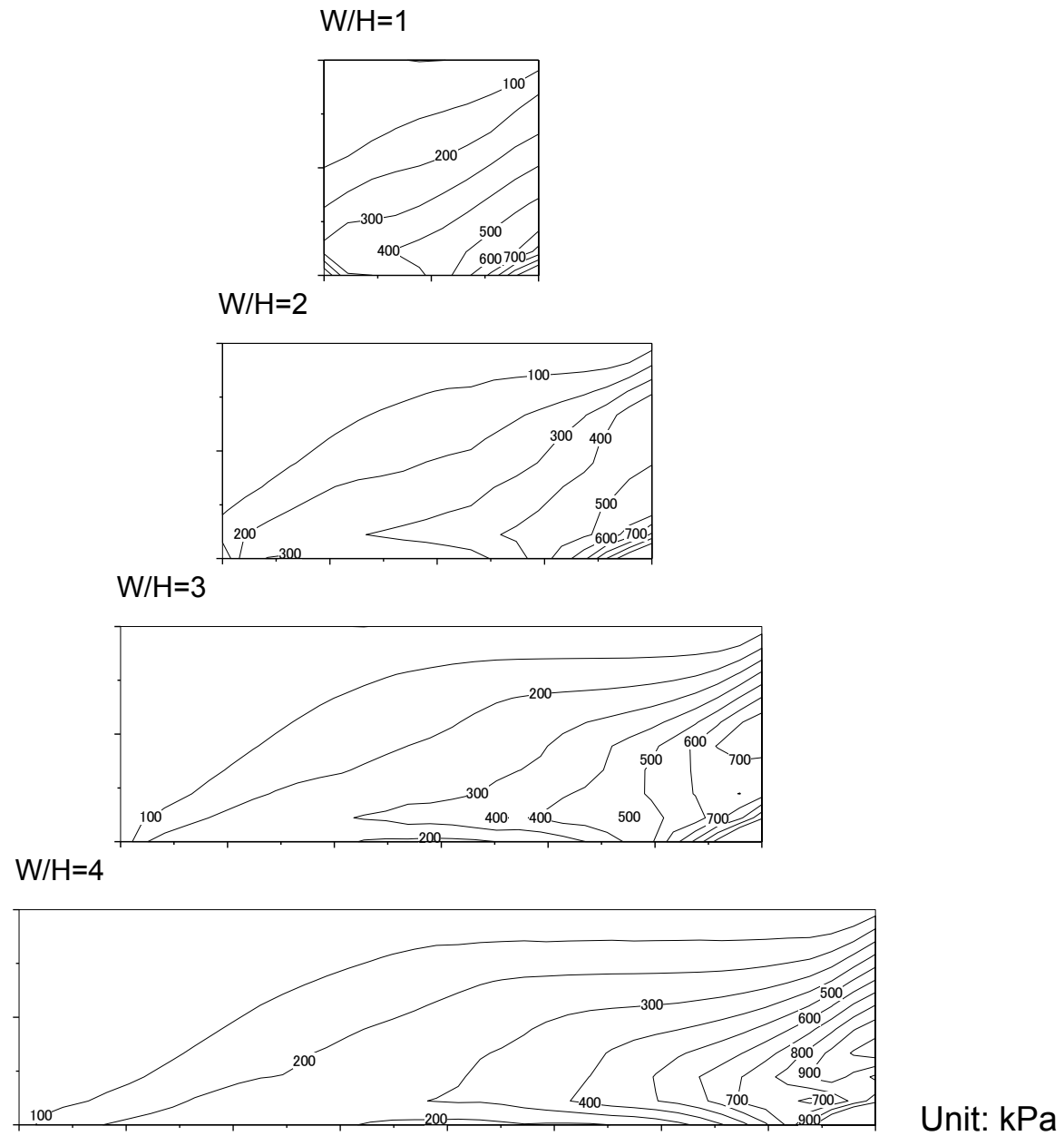
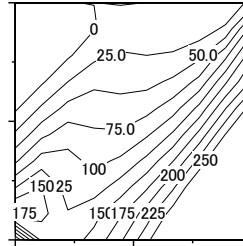


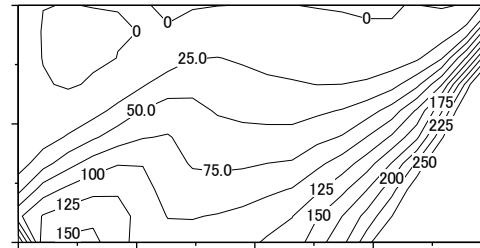
Figure 6(a) Contours of horizontal normal stress  $\sigma_x$  at the end of calculation



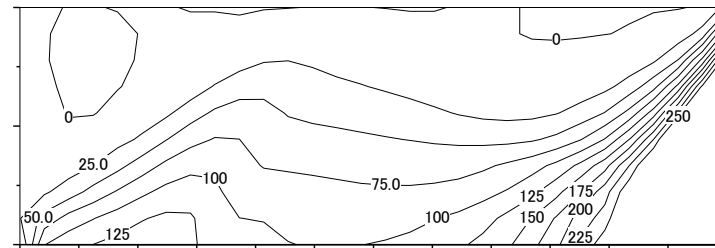
W/H=1



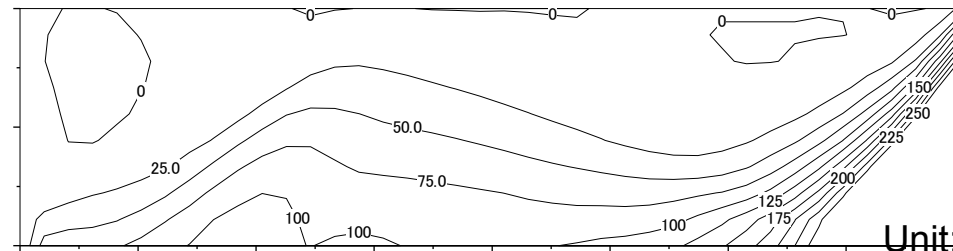
W/H=2



W/H=3



W/H=4



Unit: kPa

Figure 6(b) Contours of shear stress  $\tau_{xz}$  at the end of calculation

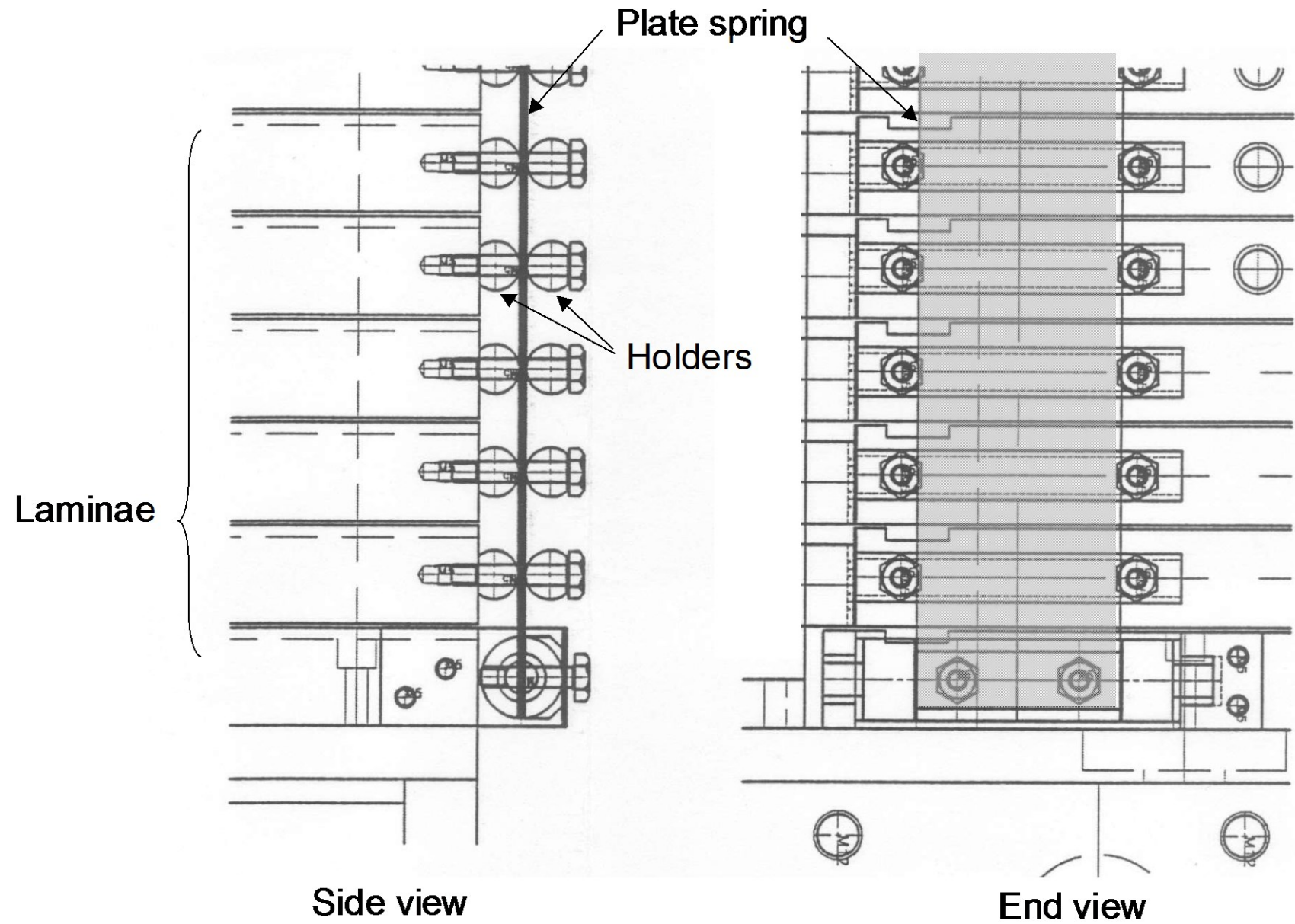


Figure 7 Detail of the plate spring and the shear sheet connection

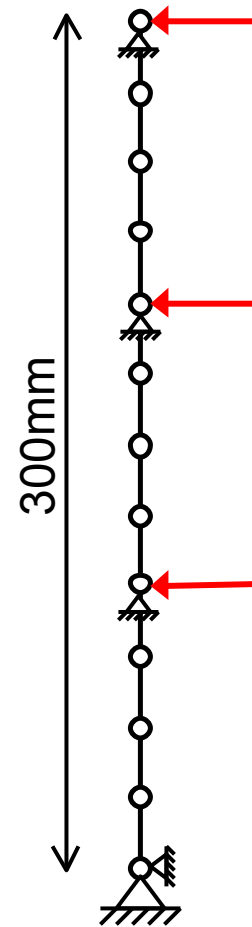


Figure 8 Typical FE mesh and the boundary condition for analysis of the plate spring

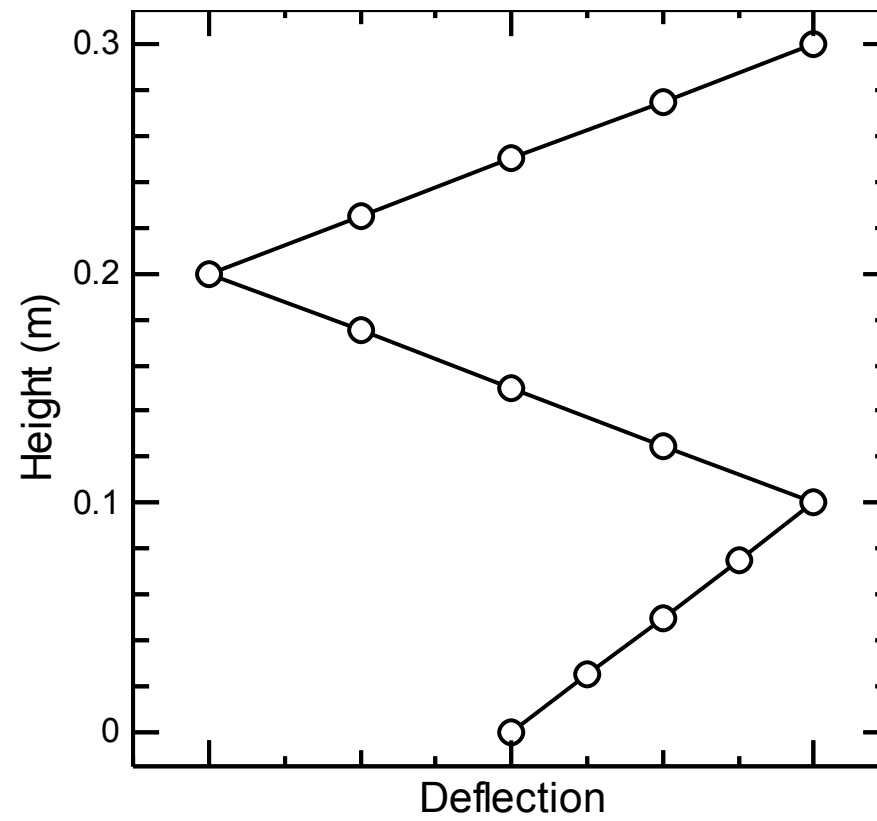


Figure 9 Natural modes of vibration of the laminar box

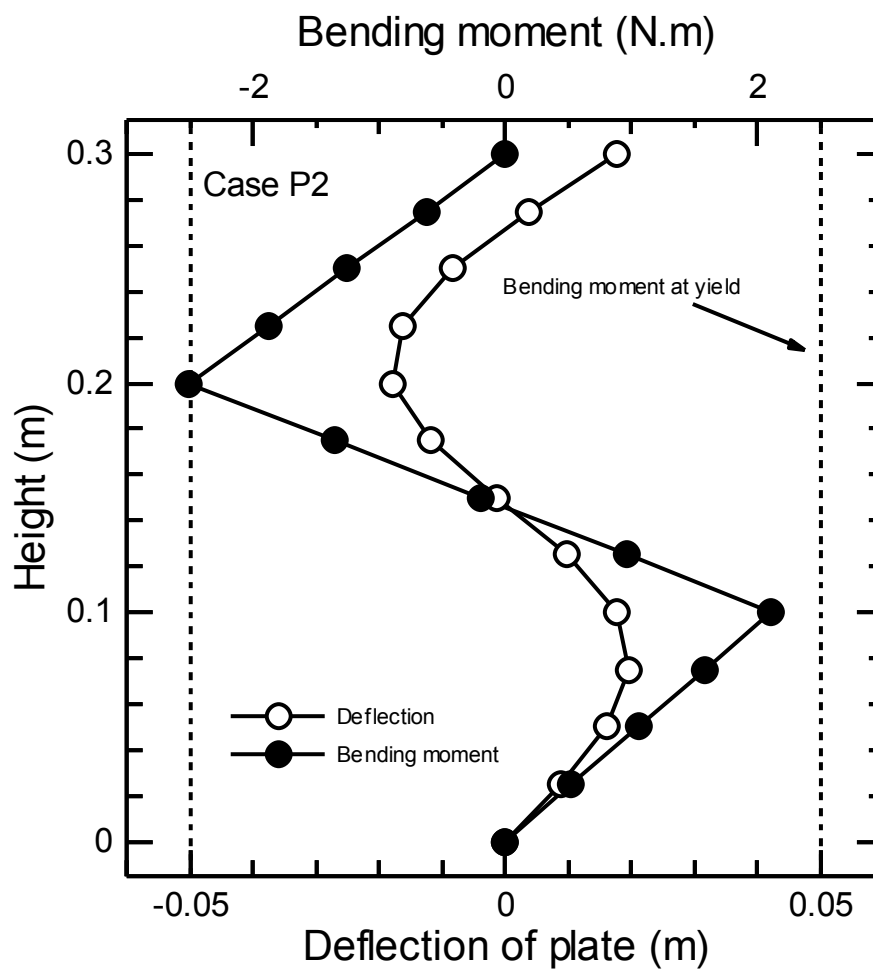
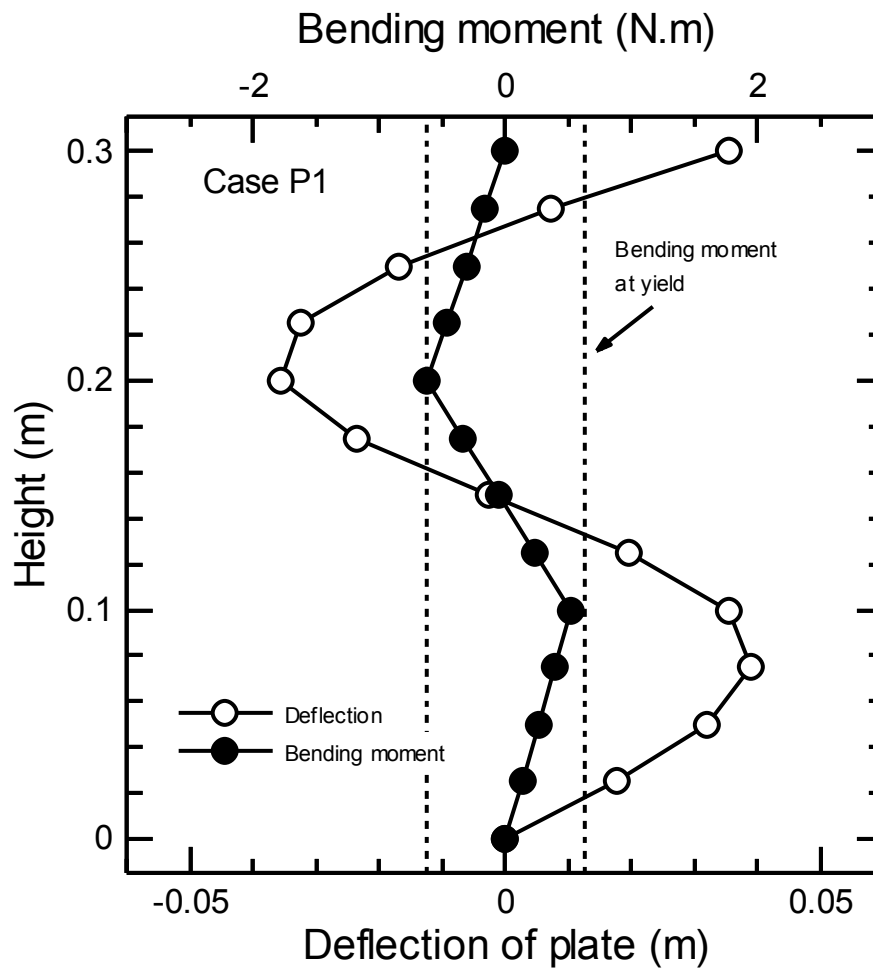


Figure 10 Calculated displacement and bending moment distributions of plate in the case of third free vibration mode

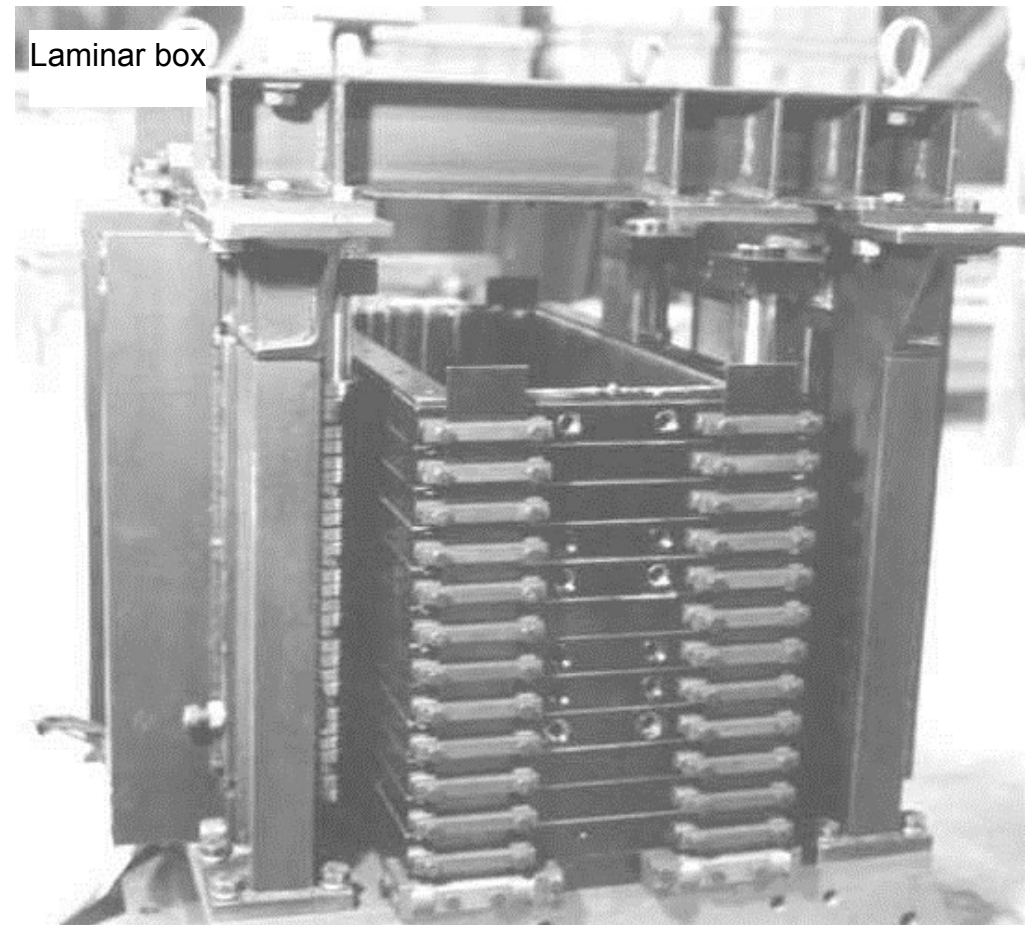
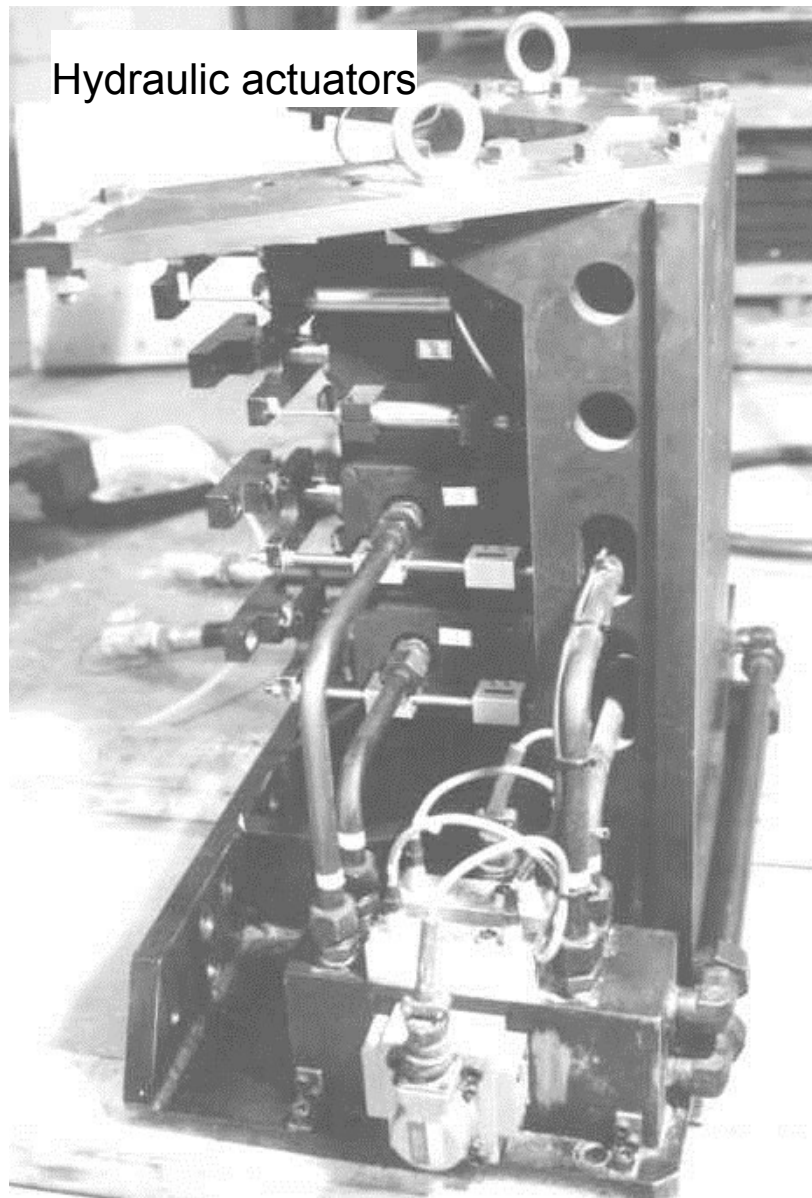


Figure 11(a) Side view of the actuators and the shear box



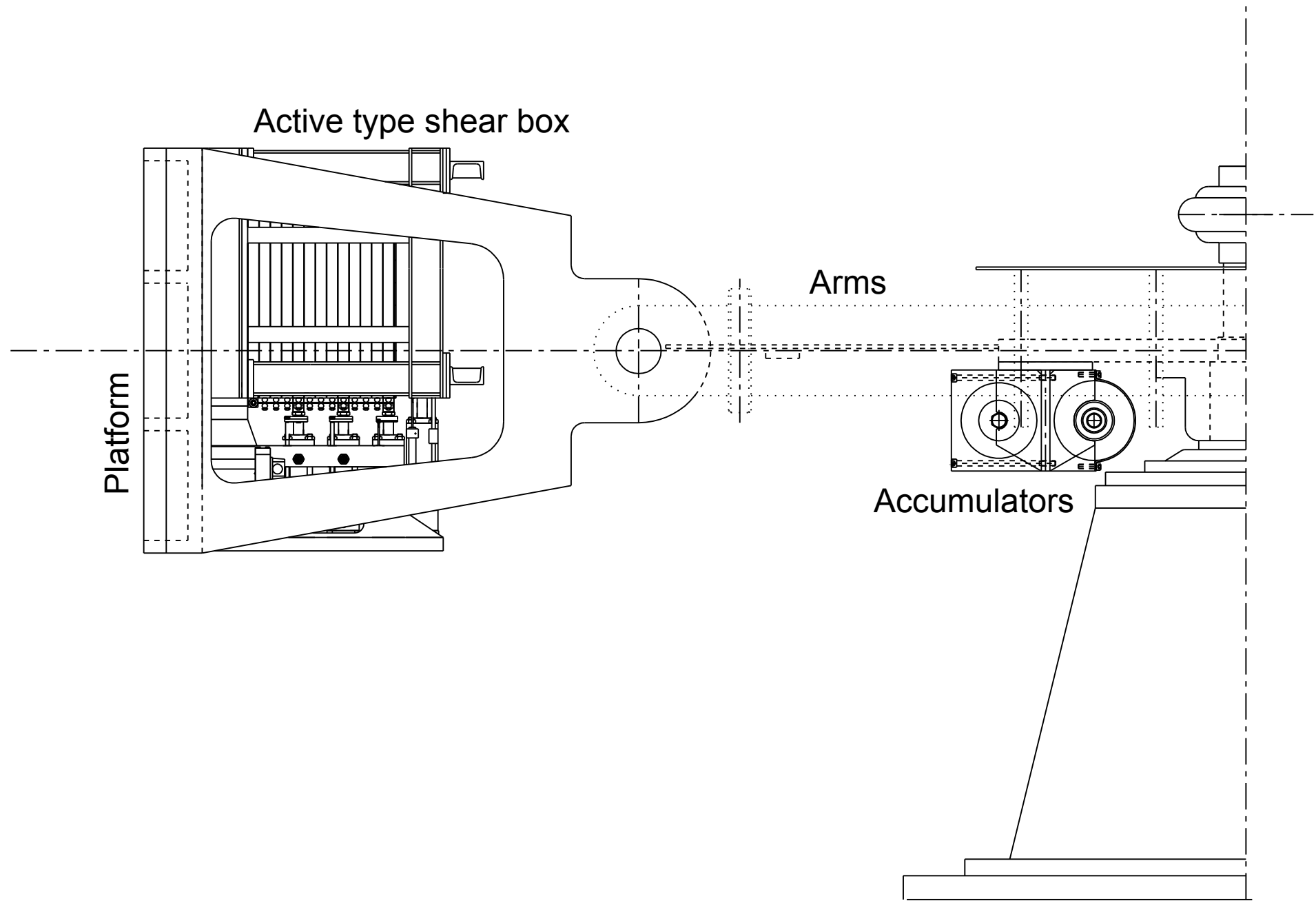


Figure 11(b) Schematic side view of the active type shear box mounted on the centrifuge

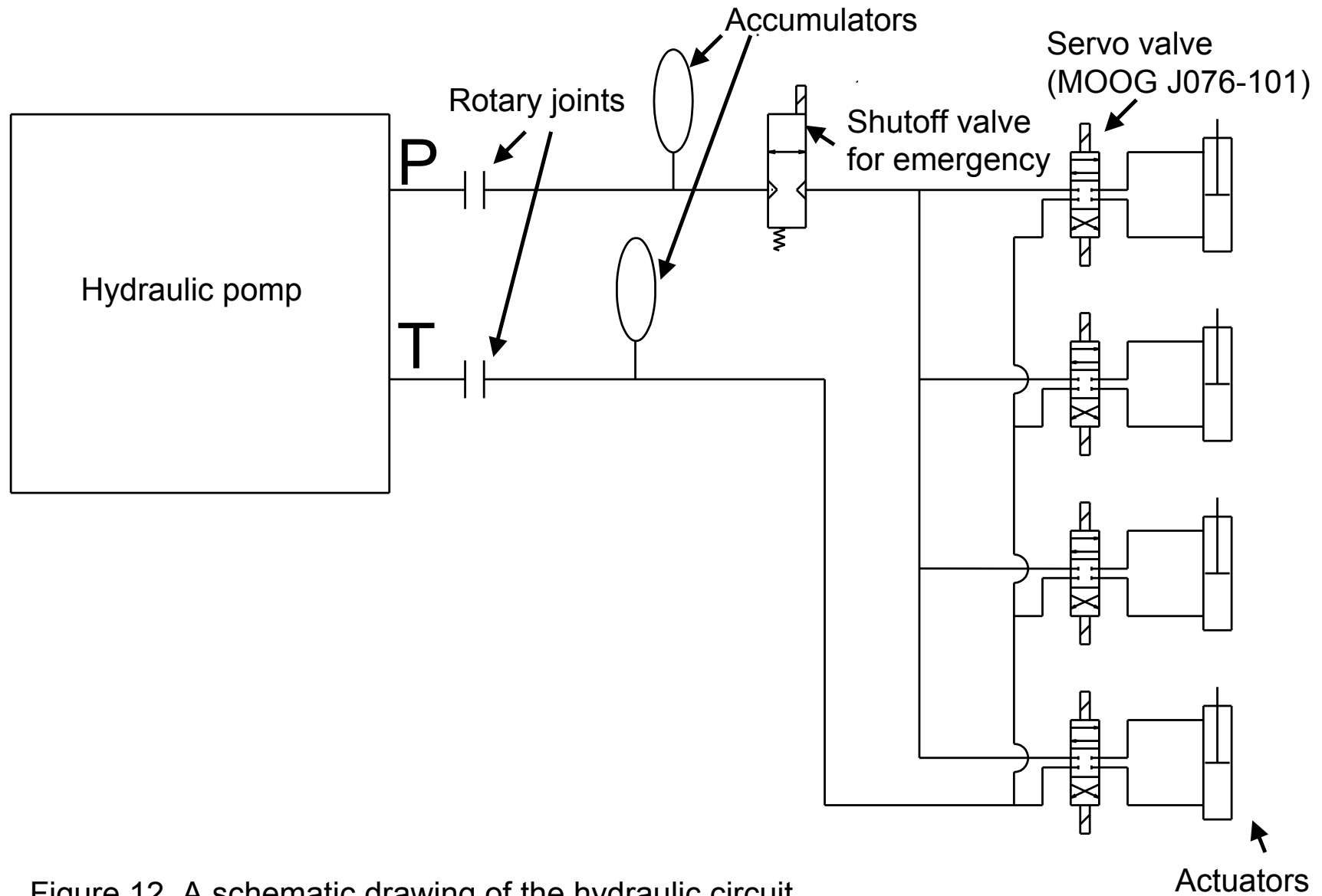


Figure 12 A schematic drawing of the hydraulic circuit

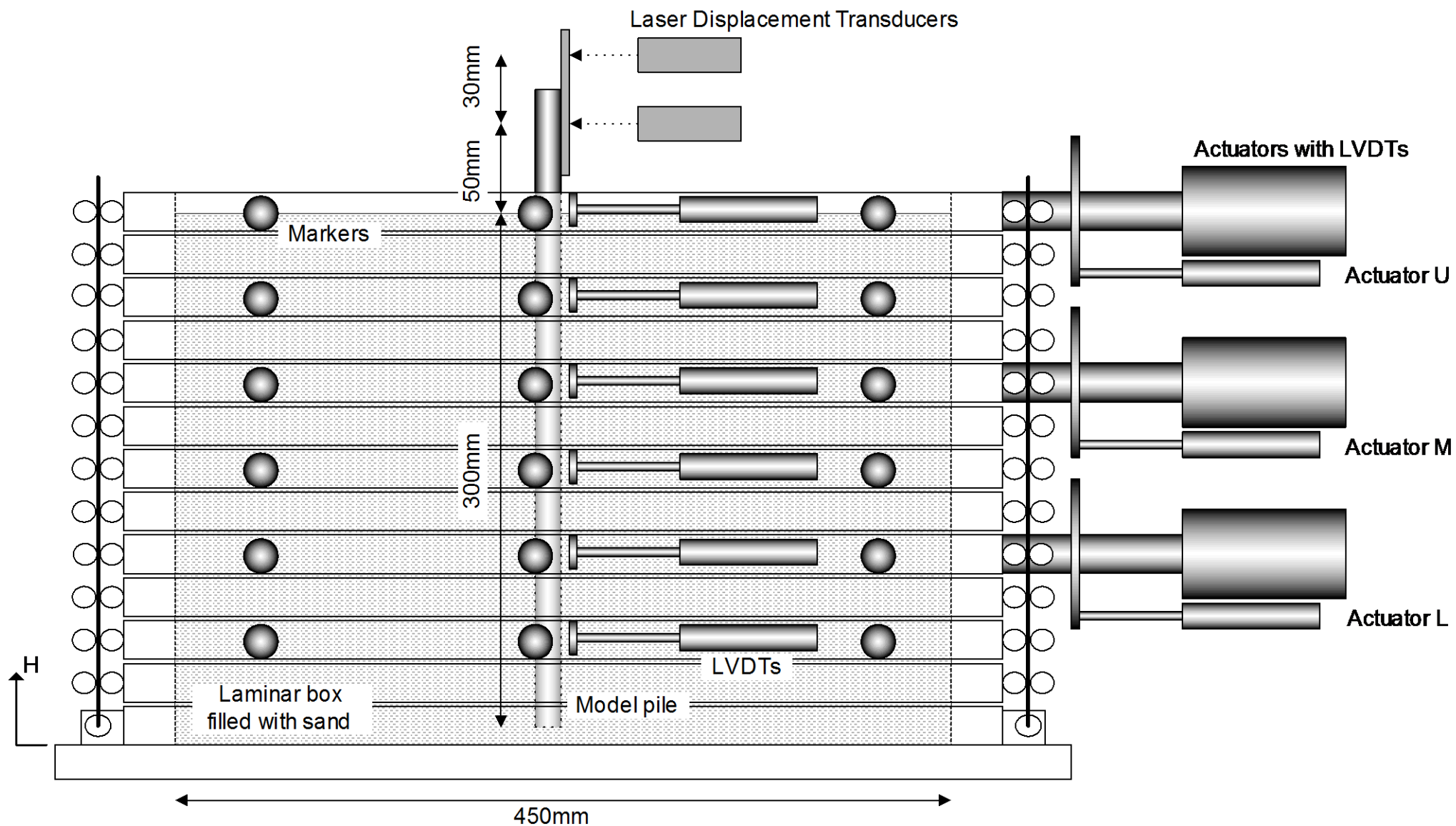


Figure 13 Instrumentation in tests

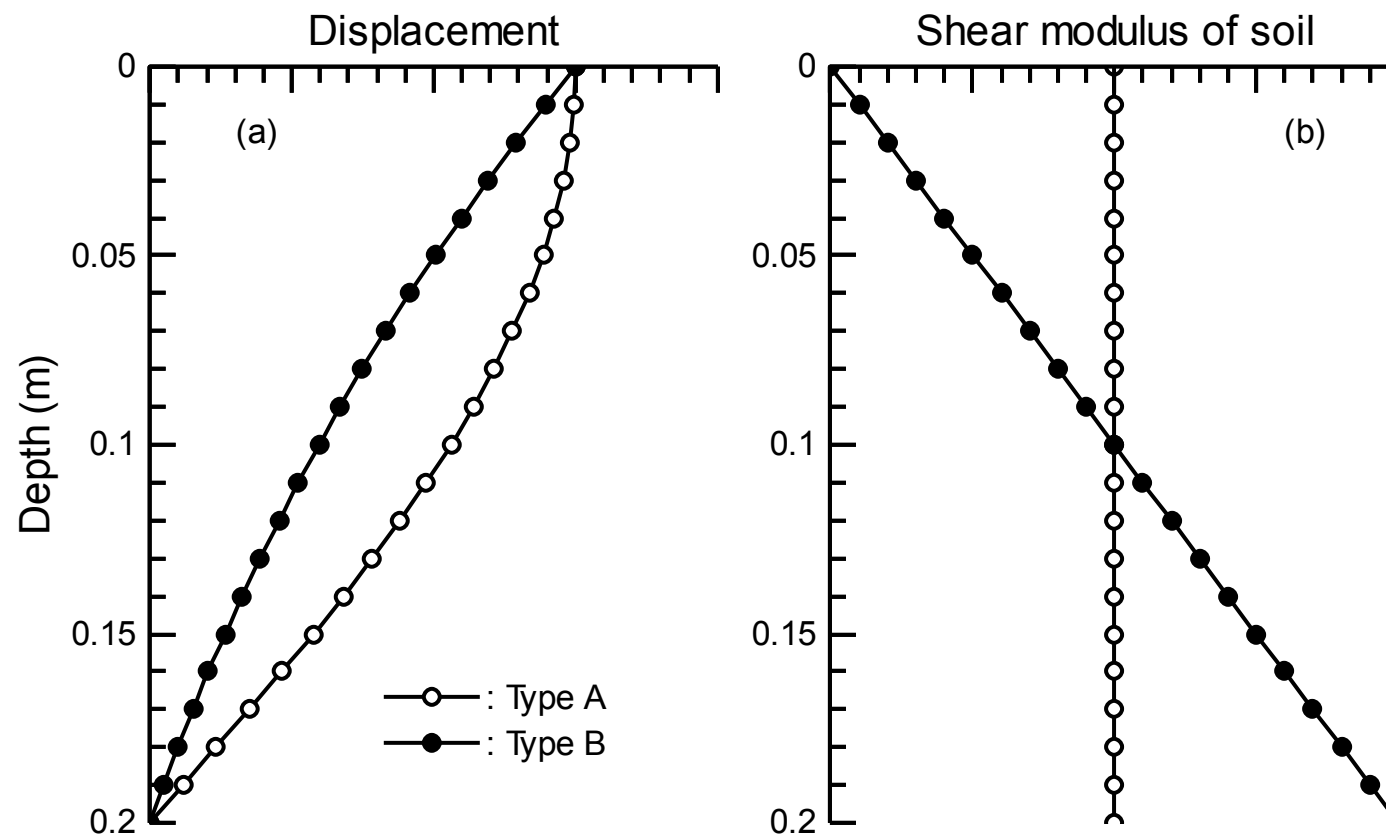


Figure 14 Two types of shear deformation mode

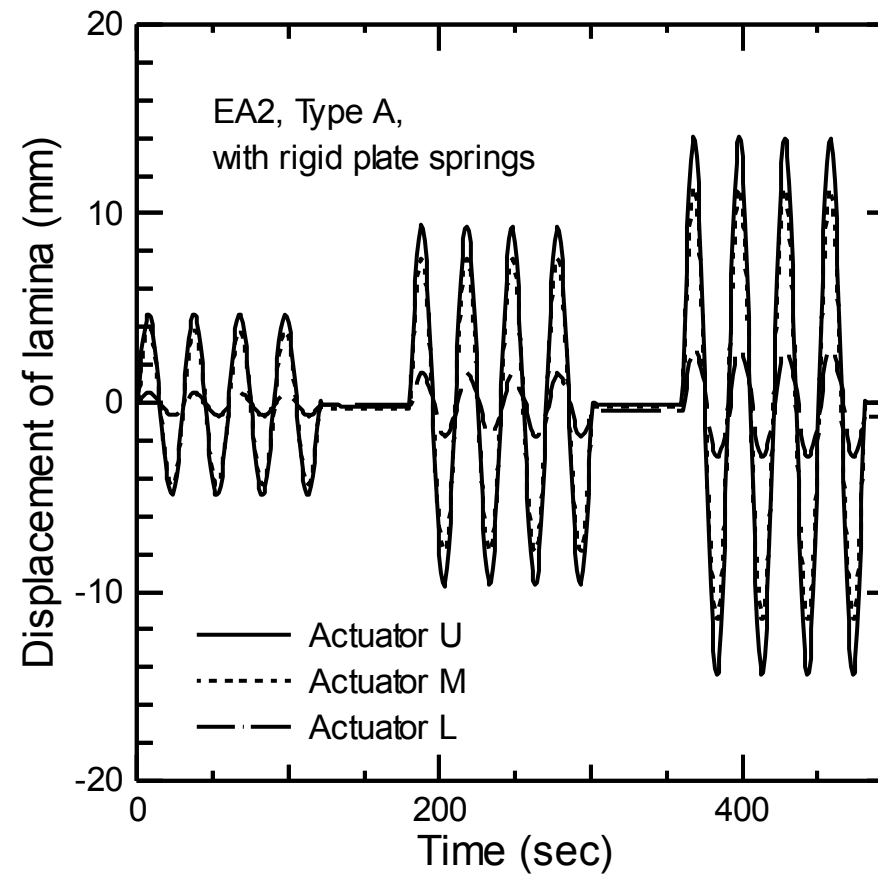


Figure 15 Typical time histories of actuator rod displacement

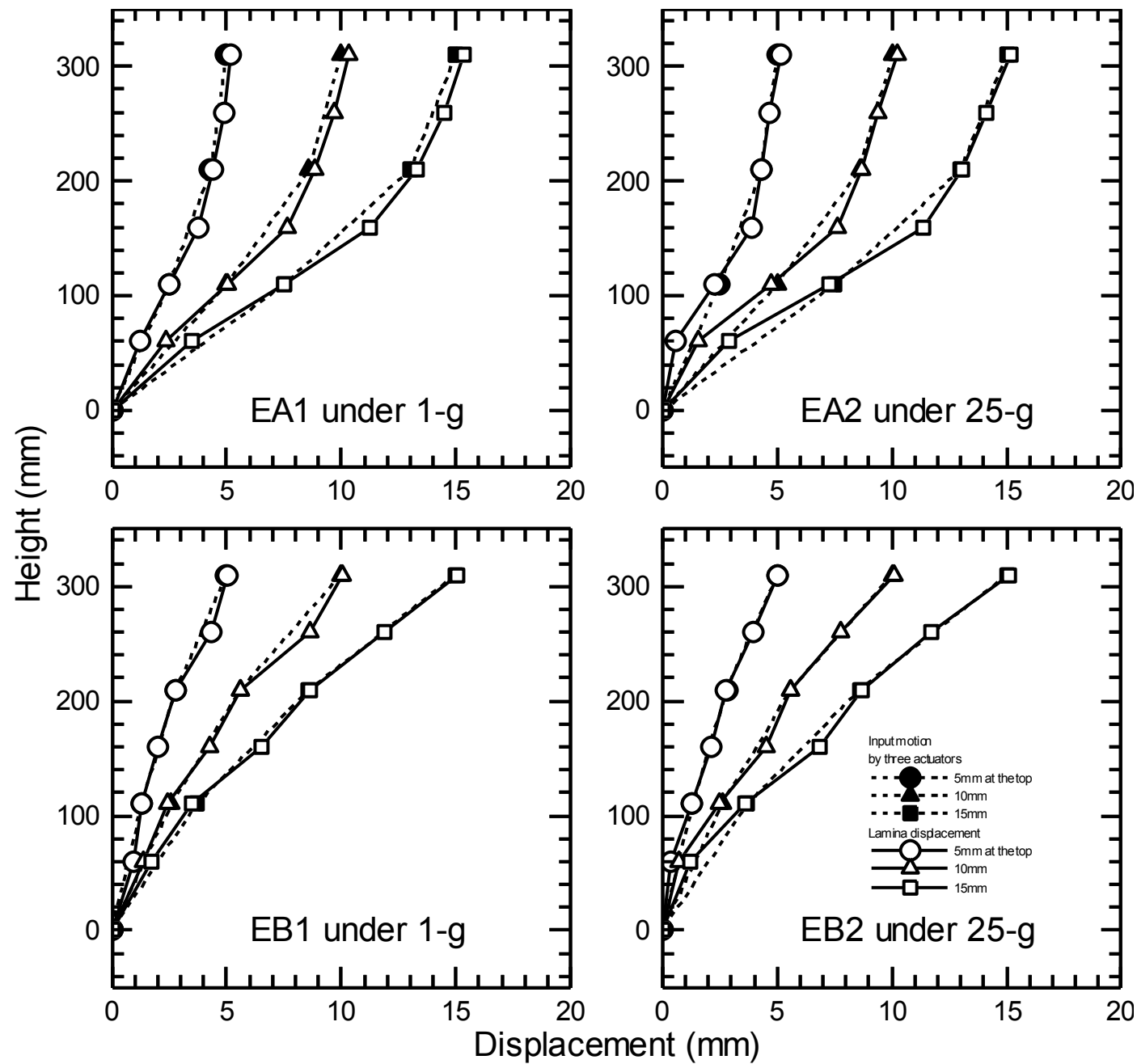


Figure 16 Observed horizontal displacement distributions of the laminae for the empty shear box



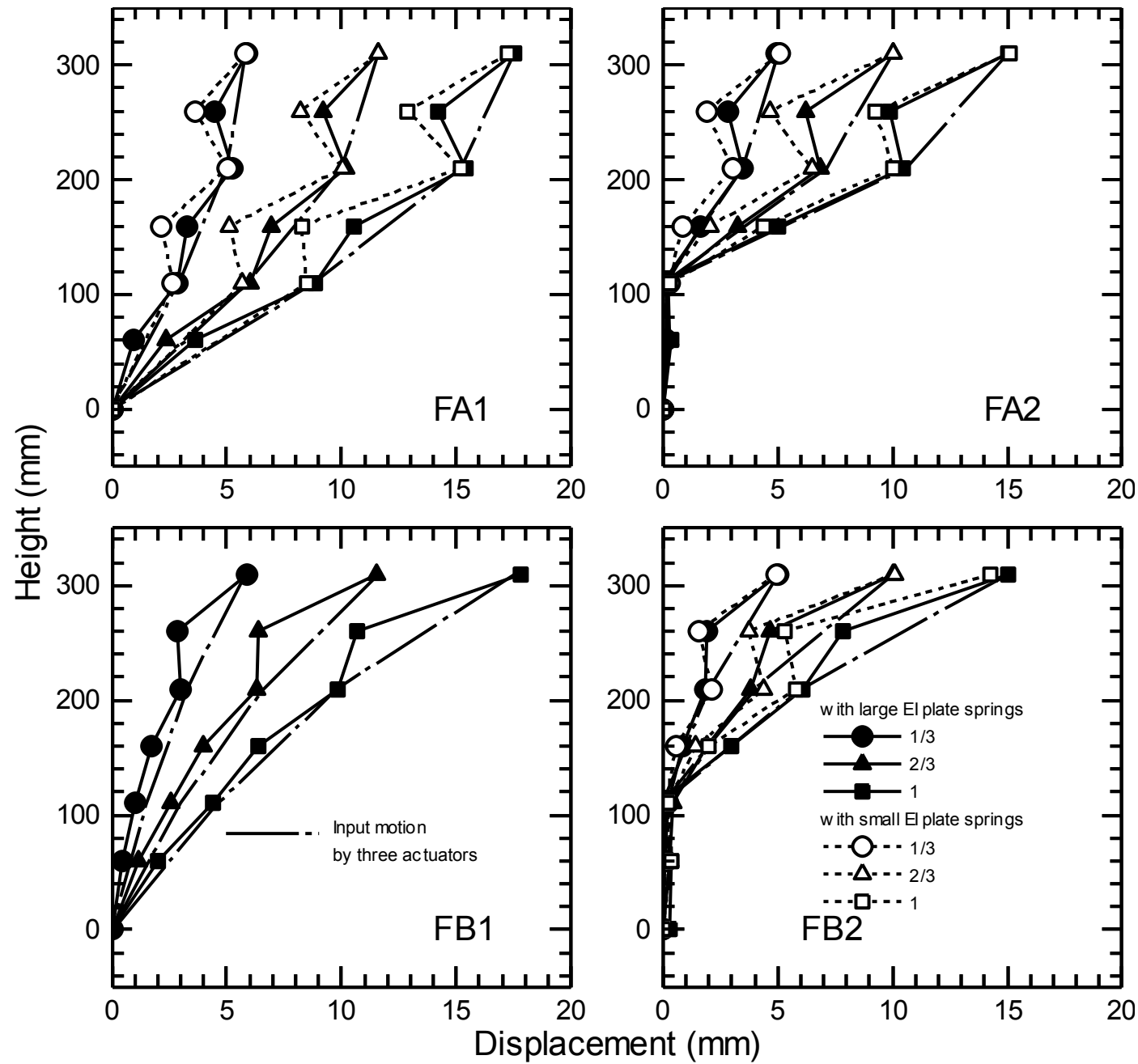


Figure 17 Observed horizontal displacement distributions of the laminae for the shear box filled with dense sand

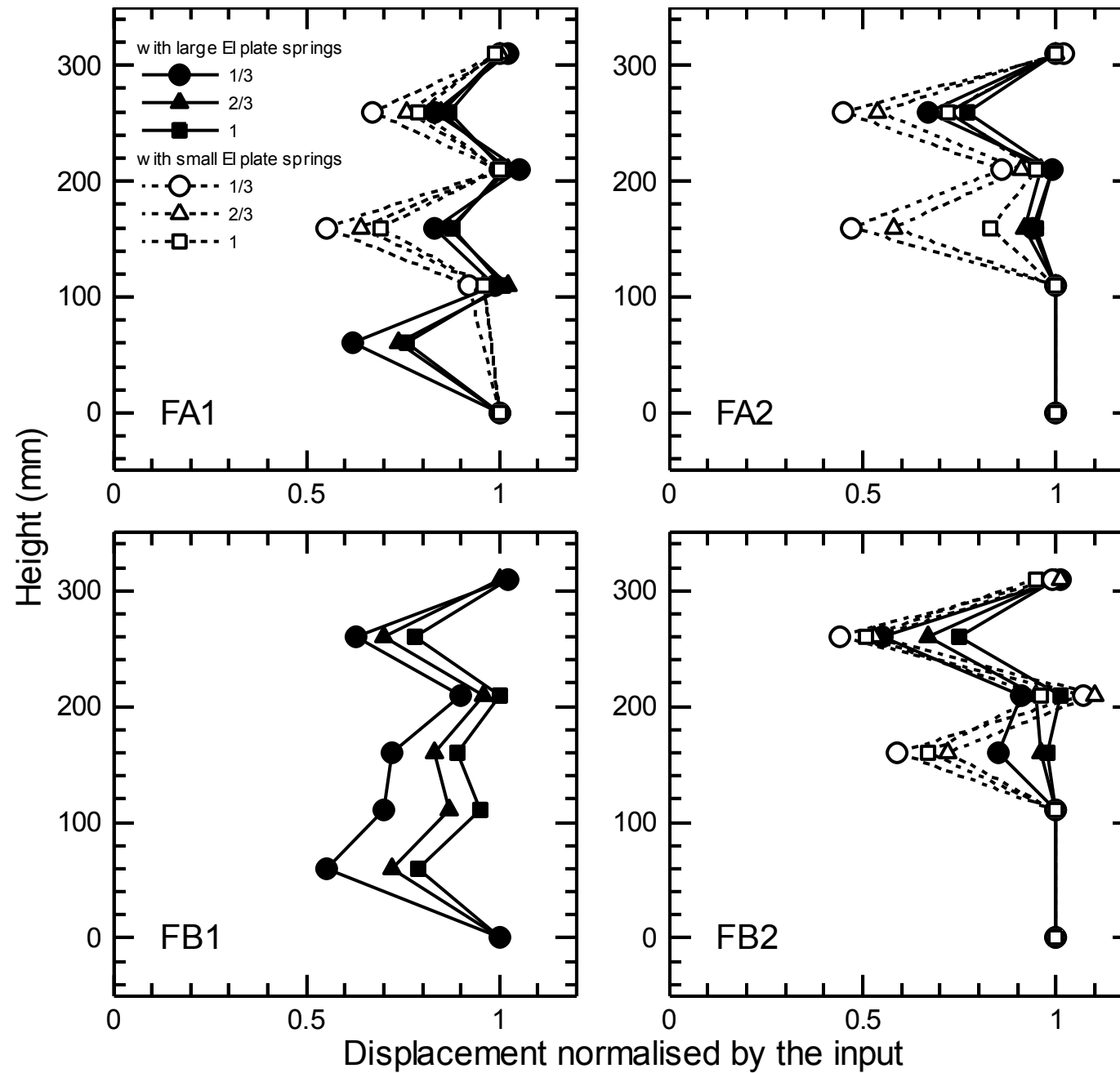


Figure 18 Normalised horizontal displacement distributions of the laminae for the shear box filled with dense sand

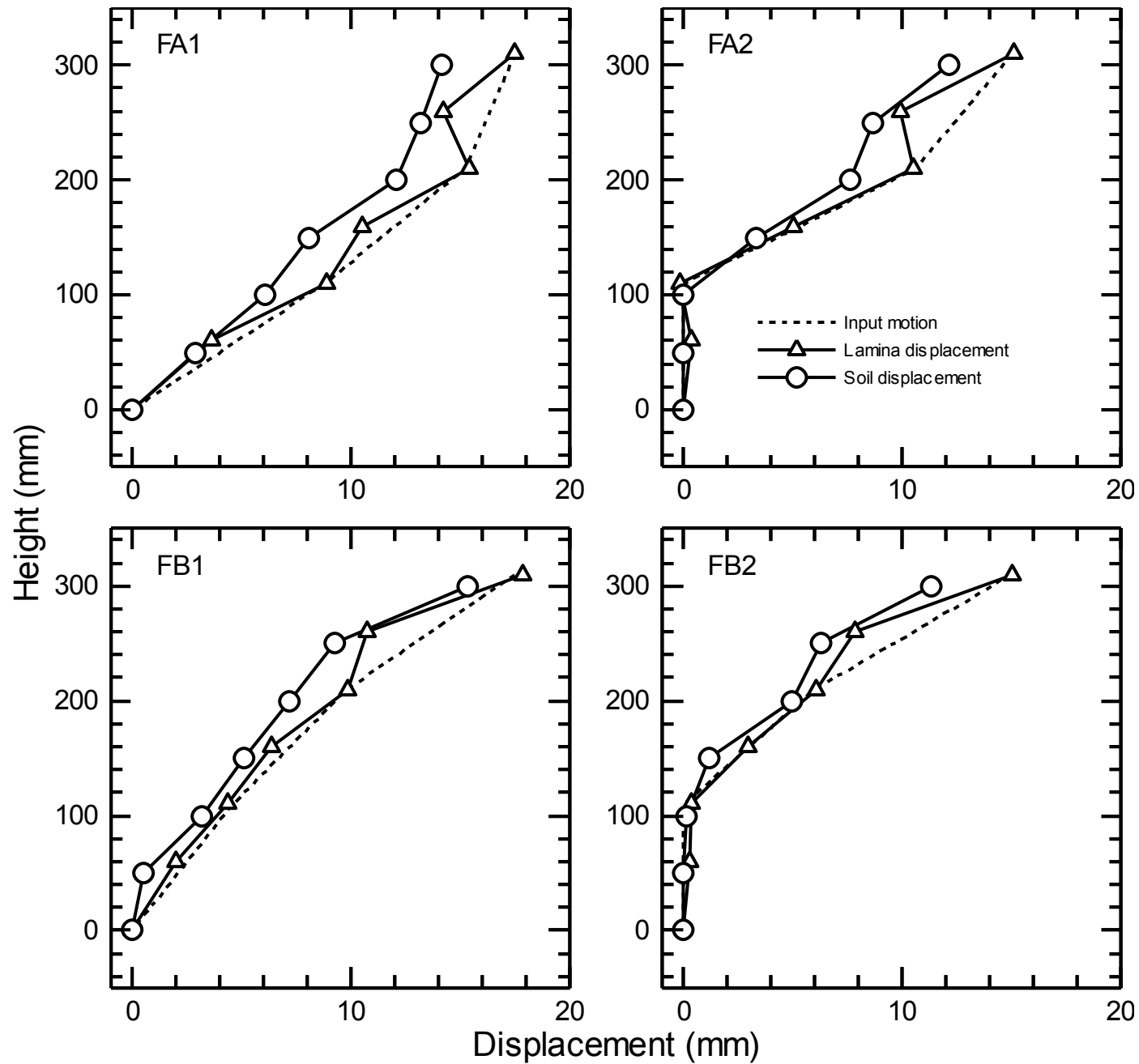


Figure 19 Observed horizontal displacement distributions of the soil, the shear box and the input value

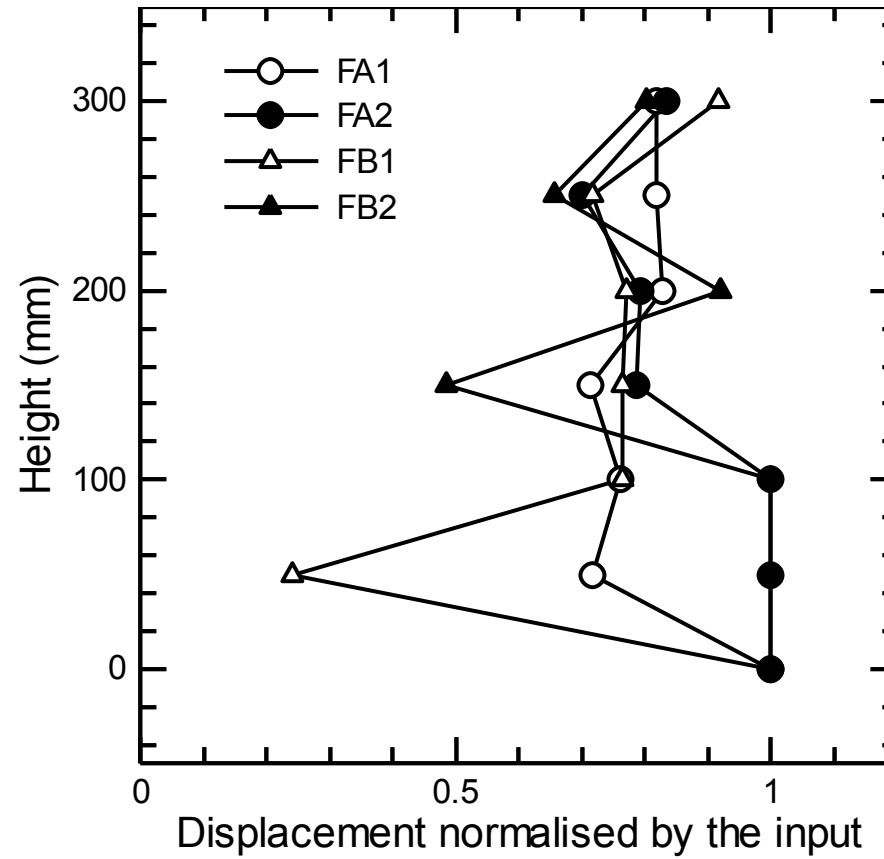


Figure 20 Normalised horizontal displacement distributions of the soil, the shear box and the input value

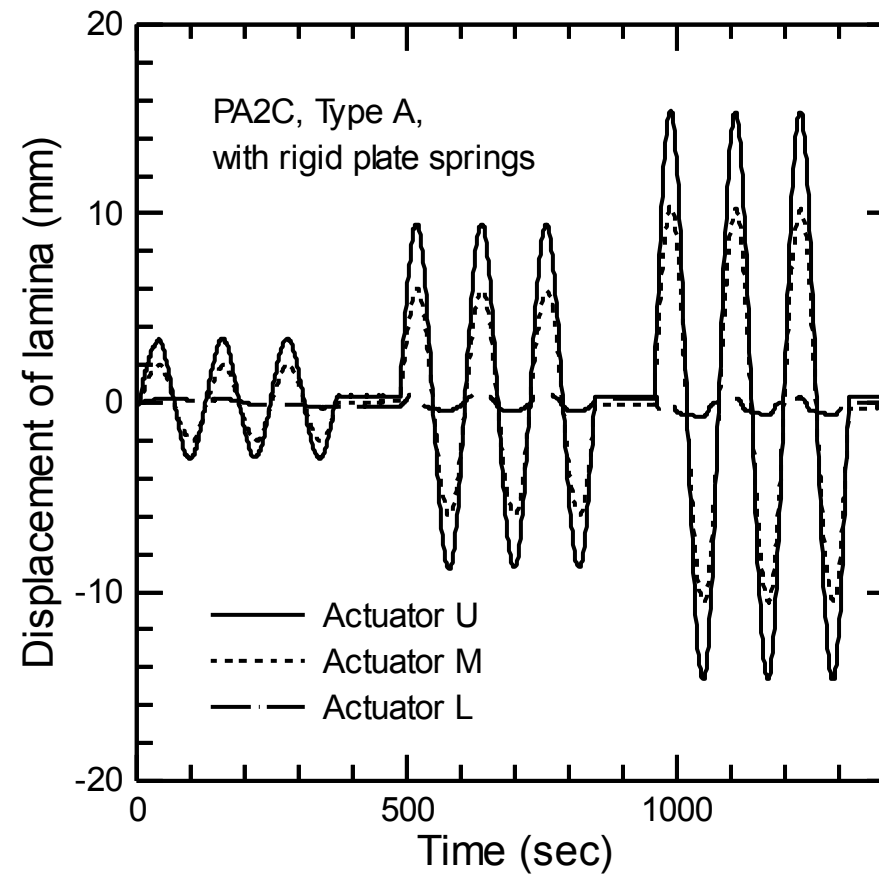


Figure 21 Typical time histories of actuator rod displacement in Case PA2C

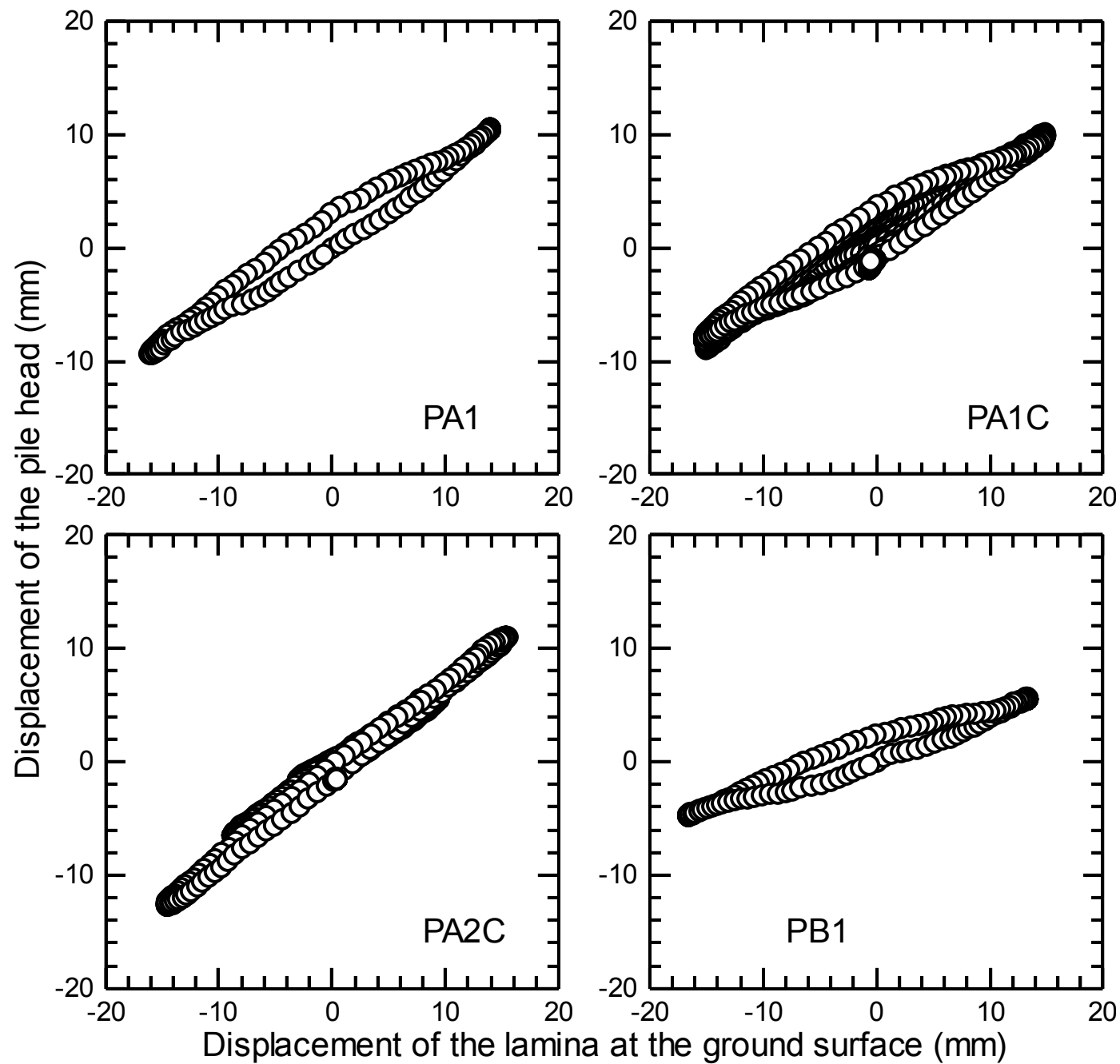


Figure 22 Relationship between observed displacements at the pile head and the input displacements of the lamina at the ground

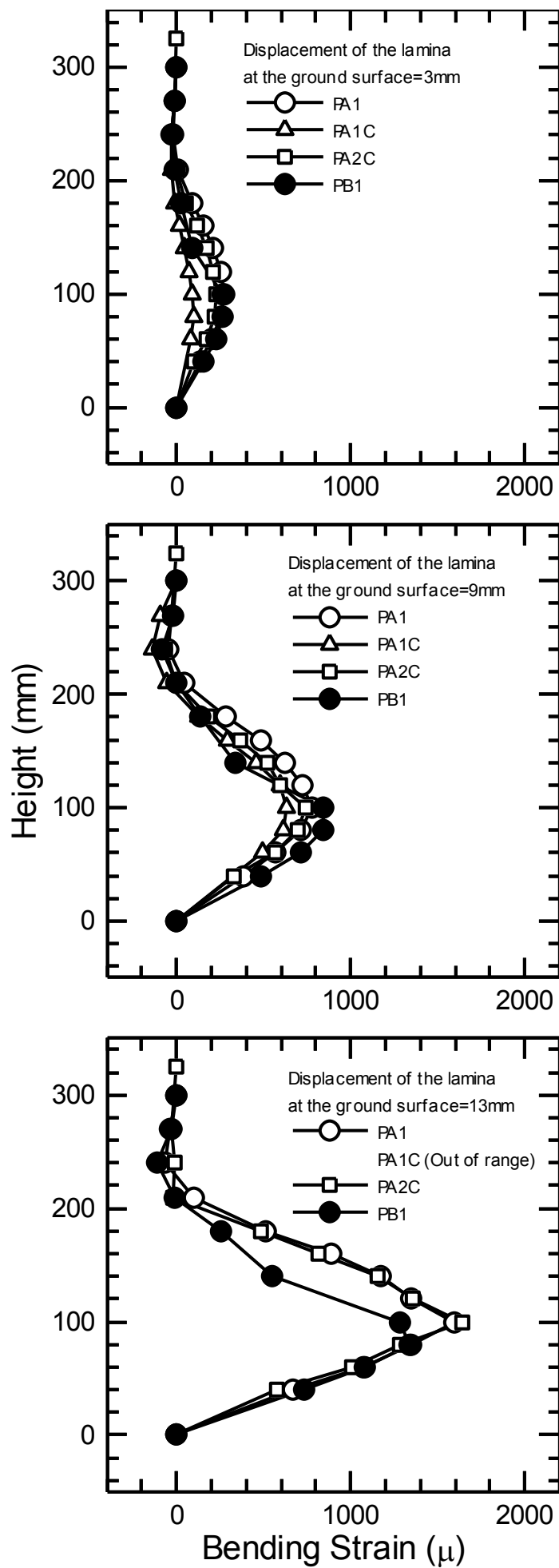


Figure 23 Observed bending strain distributions of the pile when the displacement of the top lamina reaches 3, 9 and 13mm for